PhD Thesis Summary

(5000 Words)

On

Bioactivity, phytochemical screening and synthesis of potent nanoparticle from some mangrove and weed species of south West Bengal against uropathogens.

Submitted by

SUNAYANA SAHA

SC/DOC/13-14/57

Under guidance & supervision of

Dr Mausumi Sikdar (nee Bhakta)

Associate Professor, Department of Life Sciences

Presidency University

Kolkata

2018

SYNOPSIS

1. INTRODUCTION

Medicinal plants are generating an ever increasing interest due to their effectiveness, low cost and minimum side effects associated with drugs derived from them. The Sundarban region of West Bengal constitutes different species of mangrove plants. Due to the stressful extreme habitat, different members of mangrove plants synthesize a large number of bioactive compounds which can be useful in industry and human health care. Nowadays infection from common pathogens are mostly resistant to several antibiotics which undermine their ability to control the infections. An estimate of sufferings due to Urinary Tract Infection (UTI) across the globe may rise up to 75% in female population in the next decade [2-6]. Some mangrove species found in Sundarban areas of West Bengal and some weed species found in Southern part of West Bengal are selected to investigate their antibacterial activity against epidemiologically studied two most prevalent urinary tract infecting bacteria of Eastern India – *Escherichia coli* and *Klebsiella pneumoniae* [1].

Mangrove plants are exposed to several abiotic stresses and are known to house wide array of phytochemicals and exhibit corresponding bioactivity. Reports and studies on proper exploitation of potentialities of the mangroves of Sundarban, as antimicrobial agents, are very limited. There are numerous reports on medicinally important plants of West Bengal, but reports on investigation of the antimicrobial activity or antioxidant property of economically unimportant plants or common weeds are very few. There is no concrete review on nanoparticle synthesis using these plant extracts as the sole reducing agent, as well. Isolation and determination of the pharmacological properties of the active components of herbal remedies allow for better formulation of drugs with reduced toxicity, and synthesis of more potent drugs on a commercial scale [7]. Total antioxidant activity and characterization of green synthesized metal nanoparticle have also been studied largely from medicinal plants which are the source of many beneficial components of herbal remedies, and can be used without any known detrimental effects [8]. Wide availability of these studied plants and their effectiveness against the selected uropathogens, make these plants a very promising alternative to commercial antibiotics, that are losing efficacy in the treatment of UTI.

Four common mangrove species of Jhorkhali area of Sundarban were selected for the study. And more than twenty common weed species from the local areas were screened for antimicrobial activity during the course of study. The study of antioxidant potentialities of the selected plant extracts and reduction potency were assayed. The green synthesized nanoparticles were characterized by UV-vis spectroscopy

initially, followed by X-Ray Diffraction (XRD) analysis, Fourier Transformed Infra Red Spectroscopy (FTIR), Zeta potential, Transmission Electron Microscopy (TEM) and finally Scanning Electron Microscopy (SEM). The characterization of the nanoparticles gave a detailed view of the nanoparticles- their size, shape, stability and homogeneity.

The nanoparticles along with some resistant antibiotics in synergy were tested against the clinical isolates. The cytotoxic assay of the synthesized nanoparticles were also done against RBC and the results are reported in this study.

2. OBJECTIVES

- Epidemiological study of drug resistance pattern of uropathogens in West Bengal.
- Screening of different mangrove plants and weeds with potential antimicrobial activity and potent antioxidant property.
- To synthesize nanoparticle using plant extracts.
- To determine the efficacy of synthesized nanoparticles.
- Characterization of the green synthesized nanoparticle by UV-Vis, Zeta Potential, FTIR, XRD, TEM and SEM.
- To investigate synergistic efficacy of antibiotics with the synthesized nanoparticle against the drug resistant uropathogens.
- Attempt to assay cytotoxic effect of the green synthesized nanoparticle.

3. REVIEW OF LITERATURE

In spite of several reports depicting international scenario of hospital acquired infections, epidemiological reports of nosocomial infections in India are very few and particularly of Eastern India. Risk factor analysis of community-acquired extended-spectrum-beta-lactamase-positive UTI in prior non-hospitalised patients [9] and an epidemiological data of US hospitals from 2006 to 2009, depicts UTI to be the most common healthcare associated infection [10]. Again mangroves such as *Rhizophora mucronata, Sonneratia alba* and *Exoecaria agallocha* were reported for possessing antibacterial activity against human pathogens such as *Staphylococcus aureus, Streptococcus* sp., *Salmonella typhi, Proteus vulgaris* and *Proteus mirabilis* [11]. *Avicennia marina* [12,13], *Avicennia officinalis, Bruguiera sexangula, Exoecaria agallocha, Lumnitzera racemosa,* and *Rhizophora apiculata* were evaluated against antibiotic resistant pathogenic bacteria [13]. *Suaeda maritima*, another mangrove, demonstrated antioxidant and antimicrobial activities [14].

Leaf extracts of *Biophytum sensitivum* in different solvents were studied for their antibacterial activity against several human pathogenic bacteria [15] and their activity is quite comparable with that of standard antibiotics.

The antimicrobial activities of medicinal plants are imparted by the active antioxidant components of those plants. Some reports are being published on the determination of the antioxidant activity of medicinal plants. *Aerva lantana* leaves showed high antioxidant content through various antioxidant evaluation studies like superoxide radical scavenging activity, hydroxyl radical scavenging activity, DPPH radical activity, etc. [16]. Antioxidant content and antimicrobial properties are shown *by Asparagus racemosus, Ocimum sanctum, Cassia fistula, Piper betel, Citrus aurantifolia, Catharanthus roseus,* and *Polyalthia longifolia*[17].

Green synthesized nanoparticle are an ecofriendly way of synthesizing nanoparticle. Environment friendly cell surface based stable gold nanoprisms synthesis at room temperature was done for the first time using *Penicillium citrinum* [18]. UV-vis spectroscopy and TEM imaging [18] experiments were done to characterize these gold nanoprisms. The green synthesis and characterization of ZnO nanoparticles using the leaf extracts of *Calotropis gigantean* and peel extracts of aloe vera [19] was also done [20]. Biosynthesis, antimicrobial activity and characterization of silver nanoparticle using aloe leaf extracts were done [21]. But there is lack of detailed reports on mangrove synthesized nanoparticles and their proper characterization as well as in their toxicity towards cells.

4. MATERIALS AND METHODS

4.1. Epidemiological Study Design and Area

The data were collected retrospectively from the laboratory register of the School of Tropical Medicine, Kolkata in 2014. The study period considered was from January 2008 to July 2013.

Inclusion criteria: The study included all the patients who were admitted and/or visited the out-patient department of the institute with symptoms of UTI during the study period and then had UTI confirmed by positive urine culture

Exclusion criteria: Patients having positive culture but underwent treatment with any antimicrobial within 48 h, receiving even only a single dose, were excluded from the study.

4.2. Isolation Identification and Preservation of Uropathogens

A clean-catch midstream urine specimen was collected from a patient admitted in a tertiary care hospital in Kolkata, with symptoms of UTI in a sterile wide- mouth leak-proof container to hold about 50ml specimen. The isolation, identification and preservation of the clinical isolates were done in that tertiary

care hospital, following the calibrated loop method. 10 µl of specimen was transferred on to the Mueller Hinton Agar (MHA) plate and streaked without flaming the loop (diameter 4mm) and incubated overnight at 37˚C. A specimen was considered positive for UTI when the density of the culture was $\geq 10^5$ colony-forming units (CFU)/ml. Further streaking on fresh sterile MHA plates were done to isolate single colony of uropathogens.

The single colony type cultures were identified using standard microbiological (Gram staining) and biochemical methods (Oxidase, Motility, IMViC, Nitrate Agar Slant for nitrate reduction, Triple Sugar Iron assay and Urease) up to genus/species level as/wherever applicable.

The isolated uropathogens were grown in stabs and stored at 4°C for further use. Proper care was taken, to conserve the generation number of the pathogenic strains and diminishing loss of antibiotic resistance factors.

4.3. 16s rDNA Analysis for Identification and Confirmation of Isolated Uropathogens

Genomic DNA was extracted from the culture provided by conventional method and 16S rDNA amplification was carried out with 8F and 1492R universal primer sequences. The capillary sequencing was done by ABI 3730XL Genetic Analyzer machine. The technical support was provided by GCC Biotech, Kolkata.

4.4. Preparation of Working Culture

Working cultures were prepared by adding fresh sterile Mueller Hinton Broth (MHB) on pre-cultured stabs of the test pathogens. The stabs with broth were incubated overnight at 37 °C. Following day 100 µl of the broth culture were added to 10ml of fresh sterile MHB and incubated at 37 °C for 2-3h and the absorbance were adjusted to 0.1 at 600nm which corresponds to the turbidity of 0.5 McFarland Standard [22].

4.5. Antibiotic Sensitivity Testing – Antibiogram

Antibiotic sensitivity testing was done following the Kirby-Bauer disc diffusion method according to the Clinical and Laboratory Standards Institute (CLSI) guidelines [23]. The antibiotics tested were broad-spectrum penicillin, third generation Cephalosporin, fourth generation Cephalosporin, Quinolones, Tetracycline, Macrolides, Aminoglycosides and Sulfonamides (Himedia, India). The experiment was repeated thrice and zone diameter was expressed as mean of the different assays.

4.6. Collection of Mangrove Leaves and Weed Leaves

Fresh leaves of *Avicennia alba Blume., Avicennia marina (Forssk.) Vierh., Brugeira cylindrica (Linnaeus) Blume* and *Sonneratia apetala Buch.-Ham*. were collected from the Jhorkhali region of the

Sundarban parts of West Bengal, India. The weed leaves of *Lippia nodiflora L., Chlerodendrum infortunatum (Linn)* and *Lippia alba (Mill),* were collected from local areas of Howrah, West Bengal. Many leaves were screened for their antimicrobial effectiveness (Table 3).

4.7. Preparation of Leaf Extracts in different solvents

The leaves were cleaned and washed in tap water and dried in shade for 3 weeks. Dried leaves were weighed and crushed in motorized grinder and stored in an airtight container and maintained at 4°C for further use. Dried plant dust were weighed and mixed separately with excess ethanol, 70 % methanol, acetone and water. The mixtures were kept overnight in an incubator shaker at 35 °C. Following day the mixtures were filtered through Whatman filter paper and the filtrates were evaporated in a rotary evaporator under reduced pressure to concentrate the plant extract [24] and a final concentration of 100 mg plant dust/ml of solvent was prepared. The extracts were stored at 4°C to prevent any degradation.

4.8. Screening of Antimicrobial Activity by Kirby Bauer's Disc Diffusion Method

Each sterile five mm filter paper disc were put in 100 µl of plant extracts (100mg plant dust/ml of ethanol). The discs were completely saturated with the extract and the surface was dried. Mueller Hinton Agar (MHA) plates were seeded with test clinical isolates and incubated at room temperature for 30 minutes for complete absorption of the inoculum. Plant extract discs, one control disc of streptomycin and another control disc of respective solvents for plant extracts were placed on the pre-seeded MHA plate. All the plates were incubated overnight at 37 °C. Triplicate assay of the experiment was done and result is expressed as the average of the different assays.

4.9. Determination of MIC and MBC of the plant extracts

The Minimum Inhibitory Concentration is the lowest concentration of antimicrobial agents that completely visually inhibits 99%growth of the microorganisms. The MIC of the extracts were determined by diluting the various concentrations of plant extracts (10 to 120 mg/ml). Bacterial strains were grown overnight on Mueller Hinton Broth at 37°C for obtaining young culture and adjusted to 1x 10^7 cfu/ml by standardizing with 0.5 Mc. Farland standard solution. 5ml plant extracts were added to 4.9 ml MHB and 0.1 ml inoculum. The tubes were incubated overnight and absorbance were noted the following day at 600nm [25]. Three sets of control tubes, one negative control tube containing individual plant extracts and the MHB without inoculum (antimicrobial control) and the second positive control tube containing the MHB, ethanol and the inoculum (solvent control), and the third positive control tube containing the MHB, Millipore water and the inoculum (organism control) were prepared. All investigations were done in triplicate. MIC was determined as the lowest concentration (mean of the

triplicate assays) of the extracts permitting no visible growth (no turbidity) when compared with the control tubes.

Minimum Bactericidal Concentration was determined by subculturing the MIC test dilution on sterilized MHA plates and further incubated overnight at 37ºC. The lowest concentration of MIC tubes with no visible bacterial growth on solid medium (mean of the triplicate assays) was regarded as MBC [25].

4.10. Determination of Antioxidant Activity

4.10.1. Total Phenolic Content

Total phenolic content was determined by using Folin-Ciocalteu method with gallic acid as standard [26]. The experiment was repeated thrice and results (mean of the different triplicate assays) were expressed as gallic acid equivalent /100 mg of dry weight of plant material.

4.10.2. Total Flavonoid Estimation

Total flavanoid content was determined by aluminium chloride assay [27]. The experiment was repeated thrice and results (mean of the different triplicate assays) were expressed as gallic acid equivalent /100 mg of dry weight of plant material.

4.10.3. DPPH Scavenging Activity

The 1,1-diphenyl-2-picrylhydrazyl (DPPH) radical is a stable radical which readily undergoes reduction in presence of an antioxidant. It has a maximum absorption at 517 mm. The ease and convenience of this reaction contributes to its widespread use in the free radical-scavenging activity assessment [28]. The scavenging activity of DPPH radicals by the plant extracts was examined by equating the absorbance values of the control and the experimental tubes. The lesser the absorbance, higher is the ability of the test sample to scavenge DPPH. The experiment was performed in triplicate and result is expressed (mean of the different triplicate assays) as percentage scavenging activity.

4.11. Synthesis of Silver Nanoparticle (AgNP)

1 mM aqueous $AgNO_3$ solution were prepared from $AgNO_3$ procured from Sisco Research Laboratory (SRL), India. To 5 ml of 1 mM aqueous $AgNO_3$ 5 ml of ethanolic extracts of *A. alba* leaves were added to make a final volume of 10 ml. The resulting solution was heated at 70°C for 30 minutes for complete formation of nanoparticles [29]. The formation of nanoparticles were confirmed by the characteristic peak of Ag in a UV-vis spectroscopy.

4.11.1. Antimicrobial Efficacy of the Green Synthesized AgNP.

Sterile Mueller Hinton Broth was added on pre- cultured stabs of the test pathogens and cultured overnight in incubator shaker at 37°C. This young cultures were washed and the cells were resuspended in freshly prepared sterile Mueller Hinton Broth to prepare the inoculum. The optical density of this broth were adjusted to 0.1 at 600nm corresponding to10^8cfu/mL of the test organisms [30]. One ml of the prepared broth i.e. broth containing 10^8 cfu and 1ml of the individual nanoparticles were added in 8ml of fresh Mueller Hinton Broth. Absorbance were noted immediately at 0 h and the setup were incubated overnight at 37°C. The following day absorbance was observed at 600nm to check the viability of the cells [30]. Further, 200 µl of samples from each experimental test tubes were plated individually on MHA plates to recheck the antibacterial efficacy of this green synthesized AgNP. The experiment was repeated thrice and results are expressed as an average of three experiments.

4.11.2. Characterization of the Green Synthesized Nanoparticles

The reduction of Ag^+ to Ag^0 that is formation of green synthesized silver nanoparticles were monitored and confirmed by scanning from 300nm to 700nm in UV-vis spectrophotometer. The functional groups responsible for the bioreduction were detected by FTIR analysis. The FTIR analysis (Technical support: CECRI) was carried out between 4000 and 400 cm−1 to identify the probable biomolecules of the extracts, responsible for capping and stabilizing the synthesized silver nanoparticles. The standard used for the FTIR assay was prepared by adding plant extract to Millipore water instead of $AgNO_3$ solution. Zeta potential measurements were carried out (Malvern Zeta Seizer 2000, Malvern, Technical support: IIIM) to determine the stability of AgNP. XRD – analysis was done to study the 3-D structure of the synthesized nanoparticles by X-ray diffraction instrument, (XRD, Philips, PW3710, Netherlands, Technical support: CLRI). The Anode material considered for the analysis was Cu, with wavelengths, K-Alpha1:1.540598 and K-Alpha 2: 1.544426 and ratio K-Alpha2/K-Alpha1 being 0.5. The divergence slit used was set at 2 and receiving slit was at 0.1. The generator voltage was maintained at 40 kV and tube current at 30mA. A continuous type scan was done to characterize the AgNP sample. The diffracted intensities were recorded from 35.01 degrees to 79.99 degrees 2θ angles. The shape and size of the synthesized nanoparticles were investigated by 200 keV Transmission Electron Microscopy (Technical support: SINP) and by ZEISS Scanning Electron Microscopy (Technical support: IIT, Kharagpur) analysis.

4.11.3. Antibacterial Activity of conjugated AgNP with Resistant Antibiotics in Synergy

For this study, some common broad spectrum antibiotics against which the test organisms are otherwise resistant or intermediate were chosen to investigate their synergistic efficacy with green synthesized

AgNP. The antibiotics selected were: Pipercillin-Tazobactum, Oflaxacin, Ceftazidime, Gatifloxacin, Gentamycin and Moxyfloxacin. The AgNPs and the antibiotics were mixed and incubated overnight at room temperature and centrifuged at 3000×g to completely wash away unconjugated antibiotic from the nanoparticles. Three control setups first with only MHB and inoculum, second with inoculum in presence of Ofloxacin and third with inoculum in presence of nanoparticles were studied. The sample setup consisted of inoculum in presence of Ofloxacin and AgNP in synergy. The setups were incubated overnight at 37 °C. The absorbance was measured in every 50 mins. for 600 mins. at 600nm and bacterial growth curve was plotted. The experiment was performed thrice and the result was expressed as the mean of the triplicate assay. The synergistic effect of conjugated AgNP (0.48 µg/ml – the non cytotoxic dose) with Ofloxacin (5 µg/ ml) showed the most significant result.

4.11.4. Cytotoxic Assay of the Green Synthesized AgNP against RBC

The toxicity level in RBC cells are demonstrated in this assay by study of haemocompatibility. Blood was collected from 6-week-old male BALB/c mice in a heparinized tube and red blood cells (RBC) were obtained by centrifugation at 1500×g for 5 min at 4°C. The experiment was performed according to guidelines approved by the ethical committee of IIT Kharagpur (NO.IIT/SRIC/AR/2015 date: 22.10.2015) Control samples of 0% lysis (in PBS buffer) and 100% lysis (in 0.1% Triton X-100) were employed in the experiment. Triplicate assays were performed and hemolytic effect of each treatment (average of the different triplicate assays) was expressed as percent cell lysis with respect to +ve control cells (% control) using the following formula: [(Abs_{570} of samples)/ (Abs_{570} of (+) ve control cells)] × 100.

5. Results and Discussion

(Please refer page no. **21** for "list of samples").

5.1. Epidemiological Study Design and Area

The infection report belonging to all age groups and both sexes, were reviewed in this study. Of the total culture samples (5476) analyzed, *E. coli* was the most dominant among all isolated uropathogens with a prevalence rate of 67.1%, followed by *Klebsiella* spp.(22%), *Pseudomonas* spp.(6%), *Citrobacter* spp. (2%), *Staphylococcus aureus* (1%), and *Enterococcus* spp.(1%). Remarkably, *Klebsiella* spp. infection in Eastern India is increasing rapidly with time. *E. coli* causes 80–90% of acute uncomplicated bacterial lower tract infections (cystitis) in young women. The behavior of each drug during the period 2008–2013 is also presented in this study.

Maximum susceptibility was recorded for the drugs belonging to fourth generation cephalosporins. Lesser resistance to quinolones can be explained by the fact that the resistance of *E. coli* to quinolones has remained rare until recently, since the wide spread use of quinolones as therapy for UTIs began [31, 32, 33]. Resistance to the penicillin combination against the uropathogens showed a steady increase from 2008 to 2011 followed by a slight decrease in the years 2012 and 2013. It has been reported that individual exposure to a penicillin combination like co-amoxiclav increases a risk for UTIs caused by co-amoxiclav resistant *E.coli* [34].

Klebsiella spp. from Eastern India UTI samples were maximally resistant to penicillin combination, followed by aminoglycosides and third generation cephalosporin. Studies conducted in West Bengal and around other parts of the country demonstrated consistency in *Klebsiella* spp., which presented the second highest resistance after *E. coli*, against different classes of antibiotics. Data are consistent with the findings of another Indian city (Salem, Tamil Nadu) where *K. pneumoniae* showed the highest resistance to a drug from the penicillin combination followed by aminoglycoside, gentamicin, third generation cephalosporin, ceftriaxone and ceftazidime [36].

5.2. Isolation and Identification of Uropathogens

Both the clinically isolated uropathogenic bacteria are found to be Gram negative organisms. Biochemical assays showed the first selected organism to be *Escherichia coli* and the second one to be *Klebsiella pneumoniae* (Table 1).

The uropathogens further showed best probable match with the 16S ribosomal RNA of *Escherichia coli* strain NBRC 102203 and the other clinical isolate's 16S ribosomal RNA gene matched with *Klebsiella pneumoniae* strain DSM 30104.

5.3. Antibiotic Sensitivity Testing - Antibiogram

The triplicate assay of antibiogram experiment (Table 2) illustrated the sensitivity, intermediate and resistance pattern of the test organisms. *K. pneumoniae* showed complete resistance against maximum antibiotics (Fig 1A, representative plate). Only chloramphenicol and doxycycline produced clear zone and thus showing significant susceptibility. *E.coli* showed variable resistance pattern against all the antibiotics (Fig. 1B, representative plate), with maximum antibiotics depicting intermediate pattern of sensitivity.

The antibiogram of both the test organisms showed resistance against many common drugs, thus indicating presence of large number of resistance factors in the bacteria [35, 36]. The isolated test species are multi antibiotic resistant MAR / multi drug resistant MDR urinary tract infecting human pathogens.

5.4. Antimicrobial Efficacy of the Plant Extracts

Out of all the leaves screened for antimicrobial efficacy all the mangrove plant extracts and two weed extracts – *C.inortunatum* and, *L.nodiflora* were most effective (Table 3). In the triplicate assay the plant extracts displayed bacterial inhibition patterns to varying extents depending on the susceptibility of the tested microorganisms. Only the ethanolic extracts among the other solvent extracts showed significant activity against all the test samples but all the extracts (methanol, acetone and water) failed to do so. The solvent in which the plant extract was made i.e. ethanol, was used as the control to compare the efficacy of the plant extracts. A standard positive control with antibiotic streptomycin (30 µg/ml) was also used, as a second control in this experiment. The average of triplicate assays was accounted and it showed that the ethanolic extract of *A.alba* displayed maximum zone of inhibition with a zone diameter of 14 mm against *K.pneumoniae* (Fig. 2 A, representative plate) and 16 mm against *E.coli.* (Fig. 2 C, representative plate). It was also found that, *K.pneumoniae* was totally resistant against the methanolic extracts of all the weed species. The inhibition zone of *C. infortunatum* ethanol extract against *K.pneumoniae* (Fig. 2D, representative plate).was found to be 11mm and *E.coli* to be 14 mm (Fig. 2B, representative plate).

5.5 Determination of MIC and MBC

Among all the triplicate assays of plant extracts investigated, *A.alba* showed the least MIC value at 60mg/ml against *E.coli* but 70mg/ml against *K. pneumoniae*, followed by *S.apetala* which has a MIC value of 70 mg/ ml against both the test organisms. Other extracts' MIC ranged between 70 to 80mg/ml (Table: 4).

The mean of triplicate assay of MBC of *A. alba* against both the organisms found to be 70mg/ml of the plant extracts while most of the other extracts showed same value of MIC and MBC (Table 4).

5.6. Antioxidant Activity

The amount of total phenolic content (TPC) was estimated biochemically and expressed as average of the triplicate assays performed in mg gallic acid equivalent /100 mg of dry plant leaves (Table 5).

The average of triplicate assays showed that, *L.alba* exhibited the maximum and *L. nodiflora* showed the minimum phenolic content among the weed extracts. Phenolic content varied widely among the samples ranging from 0.30 mg gallic acid equivalent/100 mg of dry leaves weight to 3.72mg gallic acid equivalent/100 mg of dry leaves weight. *A.alba* showed highest phenolic content and all the mangrove extracts represented more phenol content than the weed extracts.

Among the weed extracts, mean of the triplicate assays of flavonoid content estimated biochemically, showed *C. infortunatum* to contain maximum and *L. nodiflora* minimum flavonoid content (Table 5). The total flavonoid content varied widely among the samples and ranged from 7.44 mg gallic acid/100 mg of dry leaves to 16.68 mg gallic acid/100mg of dry leaves. All the mangrove extracts showed moderate flavonoid content.

DPPH scavenging ability of all the plant extracts in ethanol solvent system were screened. The mean value of triplicate tests exhibited that the ethanolic extract of *L.alba* depicted highest scavenging activity with a percentage of 69.9%. and the lowest scavenging activity of 47.9 % was displayed by *C. infortunatum*. All the mangrove plant extracts showed moderate to high scavenging activity in comparison with the weed extracts. *A. marina* showed highest scavenging activity, 72.84% and *B.cylindrica* the lowest with 63.52% (Table 6).

The antioxidant activity of these extracts could not be explained only on the basis of their phenolic content but also requires proper characterization of the phytochemical profile. This lack of correlation between antimicrobial efficacy and total antioxidant content of a particular plant leaf extract is in agreement with other literature [37]. It is known that only flavanoids with a certain structure and at a particularl hydroxyl position in the molecule can act as proton donating agent and show radical scavenging activity [38, 39]. This report is in accordance with the investigations reported by Sengul et al. [40], where there was no correlation between total phenolic content and antioxidant capacities of a number of medicinal plant extracts.

5.7. Antibacterial Efficacy of Synthesized AgNP

The absorbance pattern of the experimental set-up depicted lack of viability of the pathogens which had interacted with AgNPs, thus confirming antimicrobial activity of the synthesized AgNPs. The absorbance of all the tubes containing AgNPs showed lesser absorbance than the control tubes containing broth and inoculum but devoid of AgNPs. Studying the average O.D. values of triplicate analyses, it can be stated that AgNP synthesized from *A.alba* has the most significant antimicrobial efficacy than the other synthesized nanoparticles against the test organisms.

Studying the triplicate sets of MHA plates, seeded with samples from the experimental tubes showed minimum number of colonies for the sample containing *A. alba* synthesized AgNP against *E.coli* (Fig 3) and *K.pneumoniae* (Fig. 4) compared to the control tubes.

Therefore it can be stated that the green synthesized AgNP from *A.alba* could be very useful in treating urinary tract infections in both hospital acquired and community acquired infective patients, and thus can be a milestone in formulating alternative drugs employing mangrove synthesized AgNPs, particularly against multidrug resistant uropathogens. Its characterization are discussed in details.

5.8. Characterization of the Green Synthesized Nanoparticles

In this study, the *A.alba* synthesized AgNP exhibited the most considerable antimicrobial effectiveness against the test clinical isolates among the other green synthesized AgNP. So, the characterization of *A.alba* synthesized AgNP is discussed in details.

In synthesis of silver nanoparticle using the leaf extracts as the sole reducing agent the aqueous solution was observed to be dark brown to reddish brown, as there is excitation and changes in electronic energy levels due to the reduction of Ag^{+} into Ag^{0} [41]. The reddish colour formation of the nanoparticles was also observed after completion of the chemical reduction of $AgNO_3$ by sodium borohydride ($NaBH_4$) which is used as standard. Comparing the UV-vis spectra of the AgNP synthesized by the leaf extract with the UV- vis spectra of chemically synthesized AgNP it is seen that characteristic plasmon band is appearing around 420nm (Fig.5) thus confirming the formation of nanoparticles.

Comparing the spectra of the *A.alba* plant extract as standard with the spectra of synthesized AgNP bands at 3796.24, 3723.82, 3443.41, 2956.97, 2879.73, 2406.98, 2314.25, 1629.85, 1383.07, 1070.55, 562.71, 466.13cm^{-1} (Fig.6 and Fig 7) it can be stated that the band at 3796.24, 3723.82, 3443.41, cm^{-1} is assigned to the O–H stretching of H-bonded alcohols and phenols. The band at 2956.97, 2879.73 cm^{-1} is attributed to O–H stretching of carboxylic acids. The peak value at 1629.85 cm^{-1} corresponds to N-H bonded primary amines. The band at 2956.97, 2879.73 cm^{-1} corresponds to C-H stretch meant for carboxylic acids. The band at 1383.07 cm^{-1} corresponds to C-N stretching of the aromatic amine group and the bands observed in 1070.55 cm^{-1} corresponds to C-O stretching of carboxylic acids, ethers, and esters. The peak at 562.71cm^{-1} corresponds to C-H stretching of the alkene group. These investigations indicate the presence of some proteins, and secondary metabolites of *A.alba* such as alkaloids, terpenoids having functional groups of alcohols, ketones, aldehydes and carboxylic acids on the surface of the silver nanoparticles [42]. AgNPs synthesized from other leaf extracts also show involvement of secondary metabolites like alkaloids, terpenoids, etc. in the reduction process. These observations signify the term green synthesized silver nanoparticles.

The negative value of zeta potential confirms the repulsion among the particles and proves that the synthesized nanoparticles are quite stable [43]. The zeta potential value of *A.alba* synthesized AgNP found to be -27.23 ±0.32mV thus confers with the study. Thus the synthesized AgNP would be stable in the pharmaceutical preparations and also to the infection site. Dispersions with a low zeta potential value will eventually aggregate due to Van Der Waal inter-particle attractions [44]. Nanoparticles with Zeta Potential values greater than +25 mV or less than -25 mV have high degrees of stability. The zeta potential value of *A.alba* synthesized AgNP are found to fall in the negative side (-27.23 mV) which shows the efficiency of the capping materials in stabilizing the nanoparticles by providing intensive

negative charges that keep all the particles away from each other. *S.apetala* (-29.30 mV) also showed high stability. All other green synthesized AgNP showed moderate zeta potential values suggesting that these particles are stable. This is also in accordance with the result reported earlier for the colloidal nanoparticles dispersion behavior [43]. The electric charges are seemed to be strong enough to hinder agglomeration and thus provide stabilization of the nanoparticles.

The X-ray diffraction pattern of the synthesized nanoparticles by *A.alba* shows diffraction peaks at 2θ = 32.3º, 46.3º, 64.5º and 76.8º (Fig. 8), which can be indexed to (111), (200), (220) and (311) planes of pure silver respectively. This data is in accordance with the powder diffraction file (PDF) No. 04-0783 pertaining to pure silver available from the Joint Committee of Powder Diffraction Standards (JCPDS) index. Comparing the results with chemically synthesized AgNP as standard, it clearly indicates and confirms the presence of silver in the form of highly crystalline face-centred cubic (fcc) structures of silver nanoparticles. From the crystallinity index the particle type is described to be mono- crystalline [45]. The AgNP synthesized by the other leaf extracts also depicted FCC crystaline structures.

The profile, size and morphology of the synthesized silver nanoparticles were revealed with the help of 200 keV transmission electron microscopy. The TEM images established the green synthesis of silver nanoparticles. Nanoparticles synthesized from different mangroves leaf produced different TEM images with different extent of homogeneity. The nanoparticles synthesized by *A.alba* (Fig 9) are most homogeneous and spherical which conforms to the shape of SPR band in the UV-Vis spectrum with an average diameter of 71.4 nm. The green synthesized AgNP show concentric rings thus depicting a large number of crystalline nanoparticles with fairly similar orientations.

In Scanning Electron Microscopy the AgNP synthesized by *A.alba* (Fig. 10) clearly reveals smooth and spherical nanoparticles.

5.9. Cytotoxic Assay

No significant difference in hemolysis could be detected between samples and negative control after 1h of incubation, up to 1 mg/ ml concentration of the nanoparticles (Fig. 11) in all the three different sets of the same experiments. Comparing with the Triton –X control (100% lysis) it is noted that more than 15 % haemolysis could be detected in samples upto a concentration of 3.9 µg/ml. The toxicity to RBC cells are regulated in dose dependent method. The nanoparticle synthesized using *A.alba* and *S.apetala* extracts showed no cytotoxic activity at 0.48 µg/ ml and below this concentration. So, the synthesized nanoparticles are completely safe against RBCs up to a concentration of 0.48 µg/ ml. But all the other nanoparticles synthesized using *C. infortunatum, A.marina, B. cylindrical* and *S. apetala* showed cytotoxicity beyond 0.24 µg/ml.

5.10. Antibacterial Activity of conjugated AgNP with Antibiotics in Synergy

Since nanoparticle synthesized using both *A.alba* and *S.apetala* extract showed complete non toxicity at a concentration of 0.48 µg/ml, we therefore investigated the antibacterial effect of nanoparticle (0.48 µg/l) synthesized using *A.alba* and *S.apetala* extract along with antibiotics to which organisms were resistant. Though both test organisms were resistant to Ofloxacin, Ofloxacin in combination with the nanoparticles synthesized using *A.alba* and *S.apetala* extracts were found to be most promising. Although the other green synthesized nanoparticles using *C.infortunatum, A.marina* and *B.cylindrica* extracts showed satisfactory synergistic activity when used along with Ofloxacin, these results are excluded from this report due to their high cytotoxicity. The killing kinetics of *A.alba* synthesized nanoparticle, Ofloxacin and the functionalized nanoparticles along with Ofloxacin were examined against *E.coli* (Fig 12) and *K. pneumonia*e (Fig 13). The killing kinetics of *S. apetala* synthesized AgNP with Ofloxacin in synergy were also investigated against *E. coli* (Fig 14) and *K. pneumoniae* (Fig 15). The result showed an excellent synergistic effect of the conjugated nanoparticles, suggesting the possibility of their combined application to control infections caused by multi-antibiotic resistant test uropathogens. From these results it is observed that, in both the control set up (i) uropathogens without any antimicrobials (either nanoparticles or antibiotic) and (ii) uropathogens in presence of ofloxacin (4 µg/ ml) reached log phase earlier, followed by (iii) uropathogens in presence of nanoparticles only (200 mins.) but no growth was observed for (iv) uropathogens in presence of nanoparticles acting synergistically with antibiotics (Fig.12, Fig.13, Fig.14, Fig.15). This study thus indicates that the nanoparticles acting with antibiotics in synergy can inhibit resistant pathogens in a much more effective way than either nanoparticles or antibiotics alone.

6. CONCLUSION

The research work is significant and has projected lights on different areas.

From the epidemiological study it can be concluded that antibiotic resistance pattern of two principal UTI pathogens, *E. coli* and *K. pneumoniae,* in West Bengal, India, appears in general to be similar to that found in other parts of India, as well as other parts of the globe. Greater than 50% resistance was observed for penicillin combinations. Hence, these drugs should not be used in empiric treatment for UTI in Eastern India. Fourth generation cephalosporin and macrolides appears to be the first choice of drug.

The ethanolic extract of *A.alba, A.marina, B. cylindrica* and *S.apetala* among the mangroves and *L.nodiflora* and *C. infortunatum* among the weed species showed significant antibacterial activity

against the test clinical isolates- *E.coli* and *K.pneumoniae*. The scope of development of natural antimicrobials will help to decrease the negative effects of synthetic antimicrobials.

The phytochemical analysis of this study reveals that the examined leaf extracts are promising sources of potent antioxidant and may be efficient as preventive agents in some diseases and can be considered as an inexpensive natural herbal source of antioxidants in pharmaceutical, and even cosmetic and food industries.

It was also seen in this study, that the antioxidant capacity of the plant extracts observed was not exclusively for the total phenolic contents, but could also possibly be due to the presence of some other phytochemicals such as ascorbic acid, tocopherol and pigments, tannins, saponins etc. which also contribute to the total antioxidant capacity [37]. Also, measurement of phenolic content by Folin-Ciocalteu method is not an absolute measurement of the amount of total phenolic materials. Diverse phenolic compounds have different extents of antioxidant efficacies, which can be correlated to their novel structure. The extracts possibly contain different type of phenolic compounds, which have different antioxidant capacities.

The UV-vis spectroscopic analysis showed formation of nanoparticles, and so the reducing power of all the plant extracts are thus confirmed. The FTIR analysis of the plant extracts and the green synthesized AgNP suggested proteins and secondary metabolites of the mangroves which could be responsible for the bioreduction, capping and stabilization of the synthesized AgNP. The release of Ag imparts the antimicrobial potency to the green synthesized silver nanoparticles [46]. The XRD data confirms the face centered cubic structure of *A.alba* synthesized nanoparticles. On characterization by TEM and SEM, the nanoparticles showed a size of 71.4nm, with spherical morphology and substantial homogeneity. The green synthesized AgNP in combination with different antibiotics showed promising results enhancing the antibacterial activity of the antibiotics. However, further research on the plant extracts are needed to identify the active principles of the extract to pin point their reducing ability and in turn can be helpful in drug designing. The information obtained from the study of synergistic effect of the green synthesized AgNP and antibiotics can be employed in drug modification to augment their activity. The cytotoxicity of the AgNP against RBCs also showed to be safe up to a concentration of 0.48µg/ml, thus enhancing the probabilities of further productive studies on formulation of topical drugs of UTI pathogens. The above mentioned study can throw light on alternative treatment and thus prove to be very helpful in clinical sciences.

REFERENCES

1. Saha, S., Nayak, S., Bhattacharyya, I., Saha, S., Mandal, A., Chakraborty, S., Bhattacharyya, R., Chakraborty, R., Franco, O.L., Mandal, S.M. and Basak, A., 2014. Understanding the patterns of antibiotic susceptibility of bacteria causing urinary tract infection in West Bengal, India. Frontiers in microbiology, 5, p.463.
2. Epp, A., Larochelle, A., Lovatsis, D., Walter, J.E., Easton, W., Farrell, S.A., Girouard, L., Gupta, C., Harvey, M.A., Robert, M. and Ross, S., 2010. Recurrent urinary tract infection. Journal of Obstetrics and Gynaecology Canada, 32(11), pp.1082-1090.
3. Foxman, B., 2002. Epidemiology of urinary tract infections: incidence, morbidity, and economic costs. The American journal of medicine, 113(1), pp.5-13.
4. Hunstad, D.A. and Justice, S.S., 2010. Intracellular lifestyles and immune evasion strategies of uropathogenic *Escherichia coli*. Annual review of microbiology, 64, pp.203-221.
5. Mukherjee, Shriparna, and Ranadhir Chakraborty. "Conjugation potential and class 1 integron carriage of resident plasmids in river water copiotrophs." Acta microbiologica et immunologica Hungarica 54, no. 4 (2007): 379-397. Mukherjee, Shriparna, and Ranadhir Chakraborty. "Conjugation potential and class 1 integron carriage of resident plasmids in river water copiotrophs." *Acta microbiologica et immunologica Hungarica* 54, no. 4 (2007): 379-397.
6. Pouwels, K.B., Visser, S.T. and Hak, E., 2012. Effect of pravastatin and fosinopril on recurrent urinary tract infections. Journal of Antimicrobial Chemotherapy, 68(3), pp.708-714.
7. Manna, A. and Abalaka, M.E., 2000. Preliminary screening of the various extracts *of Physalis angulata* (L.) for antimicrobial activities. Spectrum J, 7(2), pp.119-125.
8. Gutiérrez, R.M.P., Mitchell, S. and Solis, R.V., 2008. *Psidium guajava*: a review of its traditional uses, phytochemistry and pharmacology. Journal of ethnopharmacology, 117(1), pp.1-27.
9. Kizilca, O., Siraneci, R., Yilmaz, A., Hatipoglu, N., Ozturk, E., Kiyak, A. and Ozkok, D., 2012. Risk factors for community-acquired urinary tract infection caused by ESBL-producing bacteria in children. Pediatrics International, 54(6), pp.858-862.
10. Agodi, A. and Barchitta, M., 2011. Epidemiology and control of urinary tract infections in intensive care patients. In Clinical Management of Complicated Urinary Tract Infection. InTech.
11. Sahoo, G., Mulla, N.S.S., Ansari, Z.A. and Mohandass, C., 2012. Antibacterial activity of mangrove leaf extracts against human pathogens. Indian journal of pharmaceutical sciences, 74(4), p.348.
12. Behbahani, B.A., Yazdi, F.T., Shahidi, F., Noorbakhsh, H., Vasiee, A. and Alghooneh, A., 2018. Phytochemical analysis and antibacterial activities extracts of mangrove leaf against the growth of some pathogenic bacteria. *Microbial pathogenesis*, *114*, pp.225-232.

13. Abeysinghe, P.D., 2010. Antibacterial activity of some medicinal mangroves against antibiotic resistant pathogenic bacteria. Indian journal of pharmaceutical sciences, 72(2), p.167.
14. Patra, J.K., Dhal, N.K. and Thatoi, H.N., 2011. In vitro bioactivity and phytochemical screening of *Suaeda maritima* (Dumort): A mangrove associate from Bhitarkanika, India. Asian Pacific journal of tropical medicine, 4(9), pp.727-734.
15. Natarajan, D., Shivakumar, M.S. and Srinivasan, R., 2010. Antibacterial activity of leaf extracts of *Biophytum sensitivum* (L.) DC. Journal of pharmaceutical sciences and research, 2(11), p.717.
16. Battu, G.R. and Kumar, B.M., 2012. In-Vitro antioxidant activity of leaf extract of *Aerva lanata* Linn. International Journal of Pharma Sciences, 2(4), pp.74-78.
17. Tsanova-Savova, S., Denev, P. and Ribarova, F., 2018. Flavonoids in Foods and Their Role in Healthy Nutrition. In Diet, Microbiome and Health (pp. 165-198).
18. Kumar, L. and Arunachalam, G., Genetic Variability in *Morus alba* L by Biochemical and Bioassay Methods for increased Silk Productivity.
19. Chaudhary, A., Kumar, N., Kumar, R. and Salar, R.K., 2019. Antimicrobial activity of zinc oxide nanoparticles synthesized from Aloe vera peel extract. SN Applied Sciences, 1(1), p.136.
20. Kaur S. and Mondal P., 2014. Study of Total Phenolic and Flavonoid Content, Antioxidant Activity and Antimicrobial Properties of Medicinal Plants. Journal of Microbiology & Experimentation, Volume 1 Issue 1.
21. Goswami, A.M. and Ghosh, S., 2013. Biological synthesis of colloidal gold nanoprisms using *Penicillium citrinum* MTCC9999. Journal of Biomaterials and Nanobiotechnology, 4(02), p.20.
22. Balouiri, M., Sadiki, M. and Ibnsouda, S.K., 2016. Methods for in vitro evaluating antimicrobial activity: A review. *Journal of pharmaceutical analysis*, *6*(2), pp.71-79.
23. Biemer, J.J., 1973. Antimicrobial susceptibility testing by the Kirby-Bauer disc diffusion method. Annals of Clinical & Laboratory Science, 3(2), pp.135-140.
24. Trifunschi, S.I., Munteanu, M.F.F., Ardelean, D.G., Orodan, M., Osser, G.M. and Gligor, R.I., 2015. Flavonoids and polyphenols content and antioxidant activity of *Ficus carica* L. extracts from Romania. Zbornik Matice srpske za prirodne nauke, (128), pp.57-65.
25. Brown, A., Smith, K., Samuels, T.A., Lu, J., Obare, S. and Scott, M.E., 2012. Nanoparticles Functionalized with Ampicillin Destroy Multiple Antibiotic Resistant Isolates of *Pseudomonas aeruginosa*, *Enterobacter aerogenes* and Methicillin Resistant *Staphylococcus aureus*. *Applied and environmental microbiology*, pp.AEM-06513.
26. Atanassova, M., Georgieva, S. and Ivancheva, K., 2011. Total phenolic and total flavonoid contents, antioxidant capacity and biological contaminants in medicinal herbs. Journal of the University of Chemical Technology & Metallurgy, 46(1).

27. Braca, A., De Tommasi, N., Di Bari, L., Pizza, C., Politi, M. and Morelli, I., 2001. Antioxidant principles from bauhinia tarapotensis. Journal of natural products, 64(7), pp.892-895.
28. Eyob, S., Martinsen, B.K., Tsegaye, A., Appelgren, M. and Skrede, G., 2008. Antioxidant and antimicrobial activities of extract and essential oil of korarima (*Aframomum corrorima* (Braun) PCM Jansen). African Journal of Biotechnology, 7(15).
29. Emeka, E.E., Ojiefoh, O.C., Aleruchi, C., Hassan, L.A., Christiana, O.M., Rebecca, M., Dare, E.O. and Temitope, A.E., 2014. Evaluation of antibacterial activities of silver nanoparticles green-synthesized using pineapple leaf (*Ananas comosus*). Micron, 57, pp.1-5.
30. Pal, S., Tak, Y.K. and Song, J.M., 2007. Does the antibacterial activity of silver nanoparticles depend on the shape of the nanoparticle? A study of the gram-negative bacterium *Escherichia coli*. Applied and environmental microbiology, 73(6), pp.1712-1720.
31. Muder, R.R., Brennen, C., Goetz, A.M., Wagener, M.M. and Rihs, J.D., 1991. Association with prior fluoroquinolone therapy of widespread ciprofloxacin resistance among gram-negative isolates in a Veterans Affairs medical center. Antimicrobial agents and chemotherapy, 35(2), pp.256-258.
32. Aguiar, J.M., Chacon, J., Canton, R. and Baquero, F., 1992. The emergence of highly fluoroquinolone-resistant *Eschericha coli* in community-acqntred urinary tract infections. Journal of Antimicrobial Chemotherapy, 29(3), pp.349-350.
33. Garau, J., Xercavins, M., Rodríguez-Carballeira, M., Gómez-Vera, J.R., Coll, I., Vidal, D., Llovet, T. and Ruíz-Bremón, A., 1999. Emergence and Dissemination of Quinolone-Resistant *Escherichia coli* in the Community. Antimicrobial agents and chemotherapy, 43(11), pp.2736-2741.
34. Leflon-Guibout, V., Ternat, G., Heym, B. and Nicolas-Chanoine, M.H., 2002. Exposure to co-amoxiclav as a risk factor for co-amoxiclav-resistant *Escherichia coli* urinary tract infection. Journal of Antimicrobial Chemotherapy, 49(2), pp.367-371.
35. Kothari, A. and Sagar, V., 2008. Antibiotic resistance in pathogens causing community-acquired urinary tract infections in India: a multicenter study. The Journal of Infection in Developing Countries, 2(05), pp.354-358.
36. Mandal, J., Acharya, N.S., Buddhapriya, D. and Parija, S.C., 2012. Antibiotic resistance pattern among common bacterial uropathogens with a special reference to ciprofloxacin resistant *Escherichia coli*. The Indian journal of medical research, 136(5), p.842.
37. Ghasemi, K., Ghasemi, Y. and Ebrahimzadeh, M.A., 2009. Antioxidant activity, phenol and flavonoid contents of 13 citrus species peels and tissues. Pak J Pharm Sci, 22(3), pp.277-281.
38. Nickavar, B., Kamalinejad, M. and Izadpanah, H., 2007. In vitro free radical scavenging activity

of five Salvia species. Pak J Pharm Sci, 20(4), pp.291-294.

39. Wojdyło, A., Oszmiański, J. and Czemerys, R., 2007. Antioxidant activity and phenolic compounds in 32 selected herbs. Food chemistry, 105(3), pp.940-949.
40. Sengul, M., Yildiz, H., Gungor, N., Cetin, B., Eser, Z. and Ercisli, S., 2009. Total phenolic content, antioxidant and antimicrobial activities of some medicinal plants. Pakistan Journal of Pharmaceutical Sciences, 22(1).
41. Dare, E.O., Makinde, O.W., Ogundele, K.T., Osinkolu, G.A., Fasasi, Y.A., Sonde, I., Bamgbose, J.T., Maaza, M., Sithole, J., Ezema, F. and Adewoye, O.O., 2012. Zinc-Salt-Mediated Synthesis, Growth Kinetic, and Shaped Evolution of Silver Nanoparticles. ISRN Nanomaterials, 2012.
42. Coates, J., 2000. Interpretation of infrared spectra, a practical approach. Encyclopedia of analytical chemistry, 12, pp.10815-10837.
43. Anandalakshmi, K., Venugobal, J. and Ramasamy, V., 2016. Characterization of silver nanoparticles by green synthesis method using *Pedalium murex* leaf extract and their antibacterial activity. Applied Nanoscience, 6(3), pp.399-408.
44. Haider, M.J. and Mehdi, M.S., 2014. Study of morphology and Zeta potential analyzer for silver nanoparticles. International Journal of Scientific and Engineering Research, 5(7), pp.381-385.
45. Gong, P., Li, H., He, X., Wang, K., Hu, J., Tan, W., Zhang, S. and Yang, X., 2007. Preparation and antibacterial activity of Fe3O4@ Ag nanoparticles. Nanotechnology, 18(28), p.285604.
46. Dwivedi, A.D. and Gopal, K., 2010. Biosynthesis of silver and gold nanoparticles using *Chenopodium album* leaf extract. Colloids and Surfaces A: Physicochemical and Engineering Aspects, 369(1-3), pp.27-33.
47. Jha, A.K., Prasad, K., Prasad, K. and Kulkarni, A.R., 2009. Plant system: nature's nanofactory. Colloids and Surfaces B: Biointerfaces, 73(2), pp.219-223.
48. Mukherjee, S. and Chakraborty, R., 2007. Conjugation potential and class 1 integron carriage of resident plasmids in river water copiotrophs. *Acta microbiologica et immunologica Hungarica*, *54*(4), pp.379-397.

List of samples

Uropathogens (selected clinical organisms):

Escherichia coli and Klebsiella pneumoniae

Leaves screened for antimicrobial efficacy:

Euphorbia hirta ,Lantana camara, Jatropha curcas, Piper betel, Justicia adhatodan , Lippia nodiflora, Lippia alba, Psidium guajava, Chlerodendrum infortunatum, Aegle marmalos, Cymbopogon citratus, Achillea millefolium, Centella asiatica, Andrographis paniculata, Avicennia alba (lanka bain), Avicennia marina, Brugeira cylindrica, Sonerratia apetala, Cassia fistula, Moringa oleifera (shojne) and *Nyctanthes arbor-tristis.*

Antioxidant potency:

Lippia nodiflora, Lippia alba, Chlendendrum infortunatum, Avicennia alba, Avicennia marina, Brugeira cylindrica and *Sonerratia apetala.*

AgNP preparation :

Chlendendrum infortunatum, Avicennia alb, Avicennia marina, Brugeira cylindrica and *Sonerratia apetala.*

Characterization of AgNP:

Chlendendrum infortunatum, Avicennia alba, Avicennia marina, Brugeira cylindrica and *Sonerratia apetala.*

Cytotoxic Assay:

Avicennia alba and *Sonerratia apetala.*

Synergistic effect of AgNP and Ofloxacin (antibiotic):

Avicennia alba and *Sonerratia apetala.*

Figure 1: Antibiogram of *E.coli* and *K. pneumoniae.*

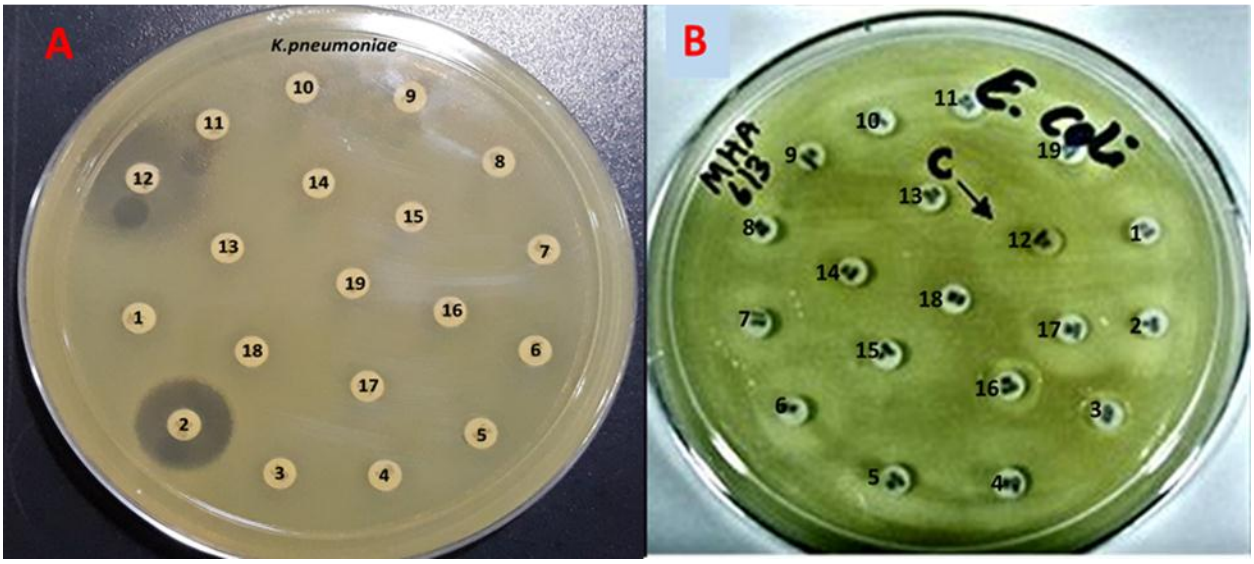

Various antibiotics produced different zone of inhibition.

Disc Number- antibiotic	Disc Number- antibiotic	Disc Number- antibiotic	Disc Number- antibiotic	Disc Number- antibiotic
1-Pipercillin/ Tazobactum	5- Oxacillin,	9- Gentamycin	13- Tobramycin	17- Moxycyclin,
2- Doxycycline	6- Levofloxacin	10- Azithromycin	14-Gatifloxacin,	18- Ticarcillin
3- Amikacin	7- Linozoid	11- Ceftriaxone	15- Meropenem	19- Ceftazidime
4- Ciprofloxacin	8- Amoxyclav,	**12- Chloramphenicol**	16- Colistin	

Fig 1A: *K.pneumoniae* showed resistance with no clear zones against maximum number of antibiotics tested. Significant clear zone were noted against doxycycline (zone diameter: 14mm) and chloramphenicol (zone diameter: 17mm) only.

Fig 1B: *E.coli* showed maximum intermediate, and fewer resistance and fewer susceptible pattern of antibiogram against the antibiotics tested in the experiment. Highest sensitivity was shown against chloramphenicol (zone diameter: 25mm).

Fig.2: Effect of antimicrobial activity of leaf extracts against *E. coli* and *K.pneumoniae.* Clear zone around the discs shows antimicrobial efficacy of the respective plant extracts.

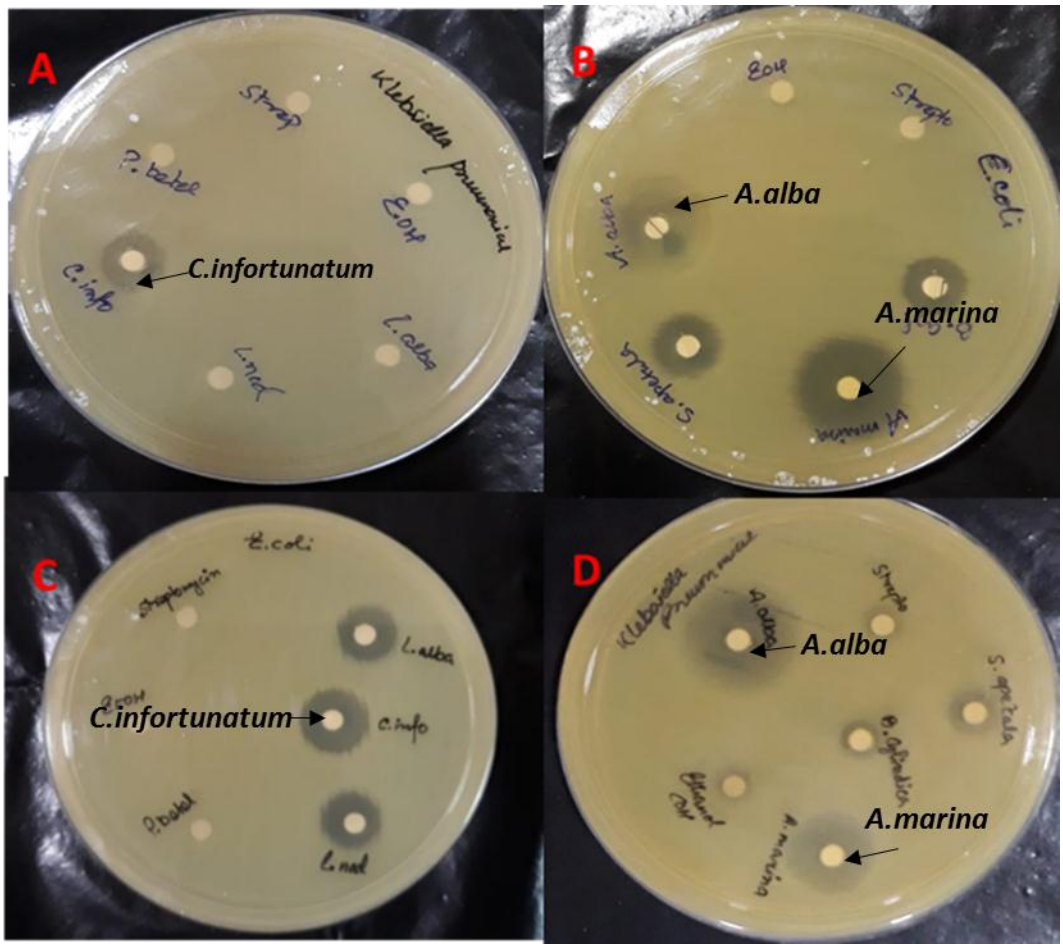

Fig. A: Effect of weed species on *K.pneumoniae- C.infortunatum* shows highest antibacterial activity with a zone diameter of 14mm.

Fig. B: Effect of mangroves on *E.coli- A. alba* (zone diameter 16mm) and *A.marina* (zone diameter 15mm) showed more antibacterial activity against *E.coli*.

Fig. C: Effect of weed species on *E. coli- C.infortunatum* shows highest antibacterial activity with a zone diameter of 11mm.

Fig. D: Effect of mangroves on *K.pneumoniae- A.alba* showed the highest activity against the test organism with a zone diameter of 14 mm.

Fig 3: Spread plate assay of AgNP synthesized by *A.alba* to determine its antimicrobial efficacy against drug resistant *E. coli.*

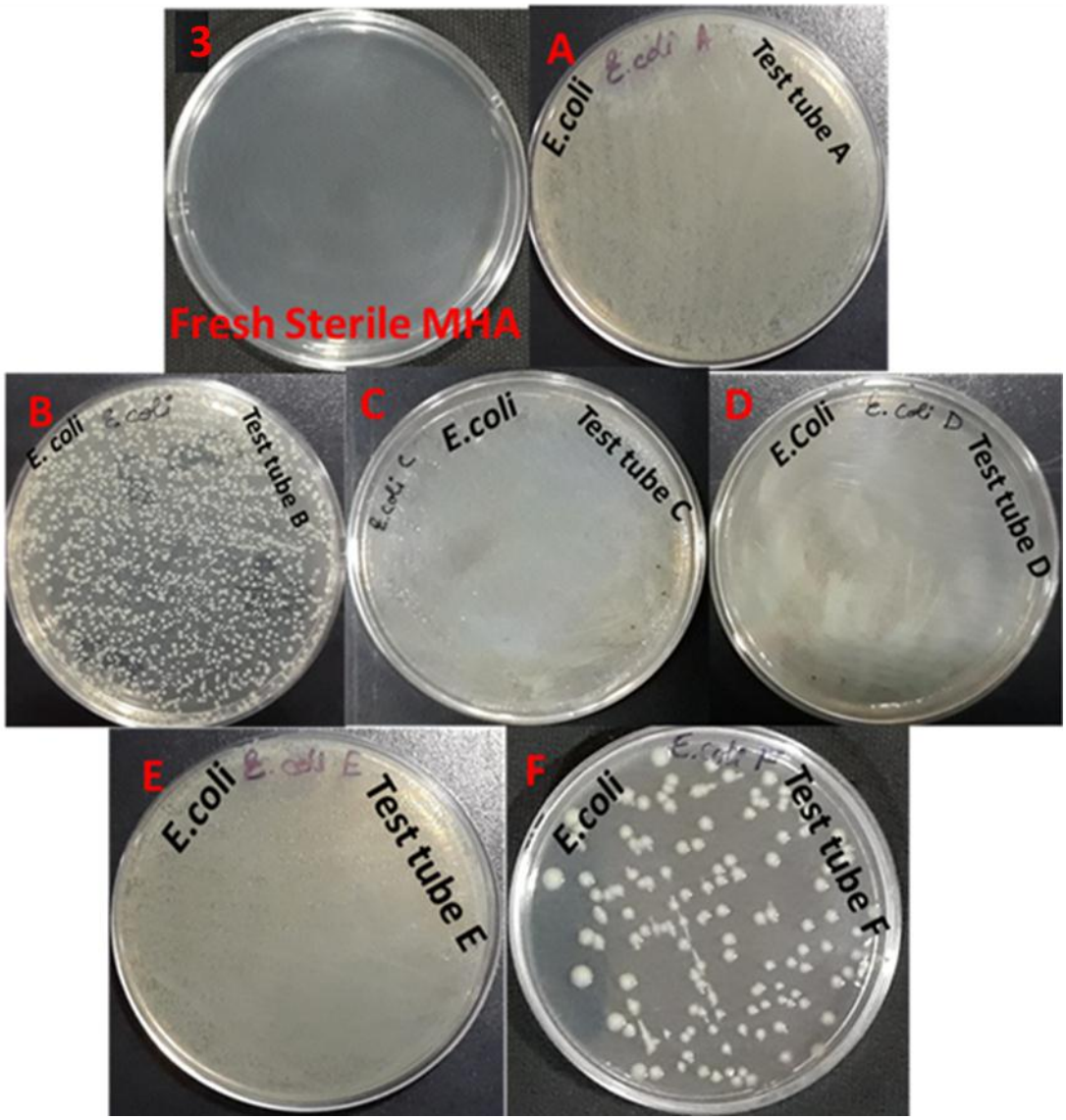

Fig 3 shows a fresh sterile Mueller Hinton Agar plate on which no colony has been grown. The translucency of this plate can be compared with the opacity of the plates with mat growth (Fig 3A, 3C, 3D and 3E).

Fig 3A shows MHA plate plated with sample from test tube A containing MHB and inoculum. This is a control set and shows profuse lawn growth of *E.coli*.

Fig 3B shows MHA plate plated with sample from test tube B containing *E.coli* with MHB and *A.alba* plant extract. This control set shows scattered growth of colonies thus indicating antibacterial efficacy of the plant extract.

Fig 3C shows MHA plate plated with sample from test tube C containing MHB, *E.coli* and ethanol (solvent used for extraction of *A.alba*) This solvent control set shows extensive mat growth of *E.coli*.

Fig 3D shows MHA plate plated with sample from test tube D containing MHB, *E.coli* and Millipore water (used for dissolving $AgNO_3$). This control set shows abundant growth of *E.coli*.

Fig 3E shows MHA plate plated with sample from test tube E containing MHB, *E.coli* and 1 mM $AgNO_3$ solution. This control set shows extensive lawn growth of *E.coli*.

Fig 3F shows MHA plate plated with sample from test tube F containing MHB, *E.coli* and *A.alba* synthesized AgNP. This test sample set shows significantly less growth of *E.coli* thus indicating high antibacterial efficacy of *A.alba* synthesized AgNP.

Image	Plate description	Volume of inoculum	No. of colonies
3	Fresh sterile MHA plate	200µl	Nil
A	Only *E.coli* inoculum	200µl	Lawn
B	**Plant extract and inoculum**	200µl	**1490±53**
C	Ethanol and inoculum	200µl	Lawn
D	Millipore water and inoculum	200µl	Lawn
E	1mM $AgNO_3$ and inoculum	200µl	Lawn
F	**AgNP and inoculum**	200µl	**54±4**

Fig 4: Spread plate assay of AgNP synthesized by *A.alba* to determine its antimicrobial efficacy against drug resistant *K.pneumoniae.*

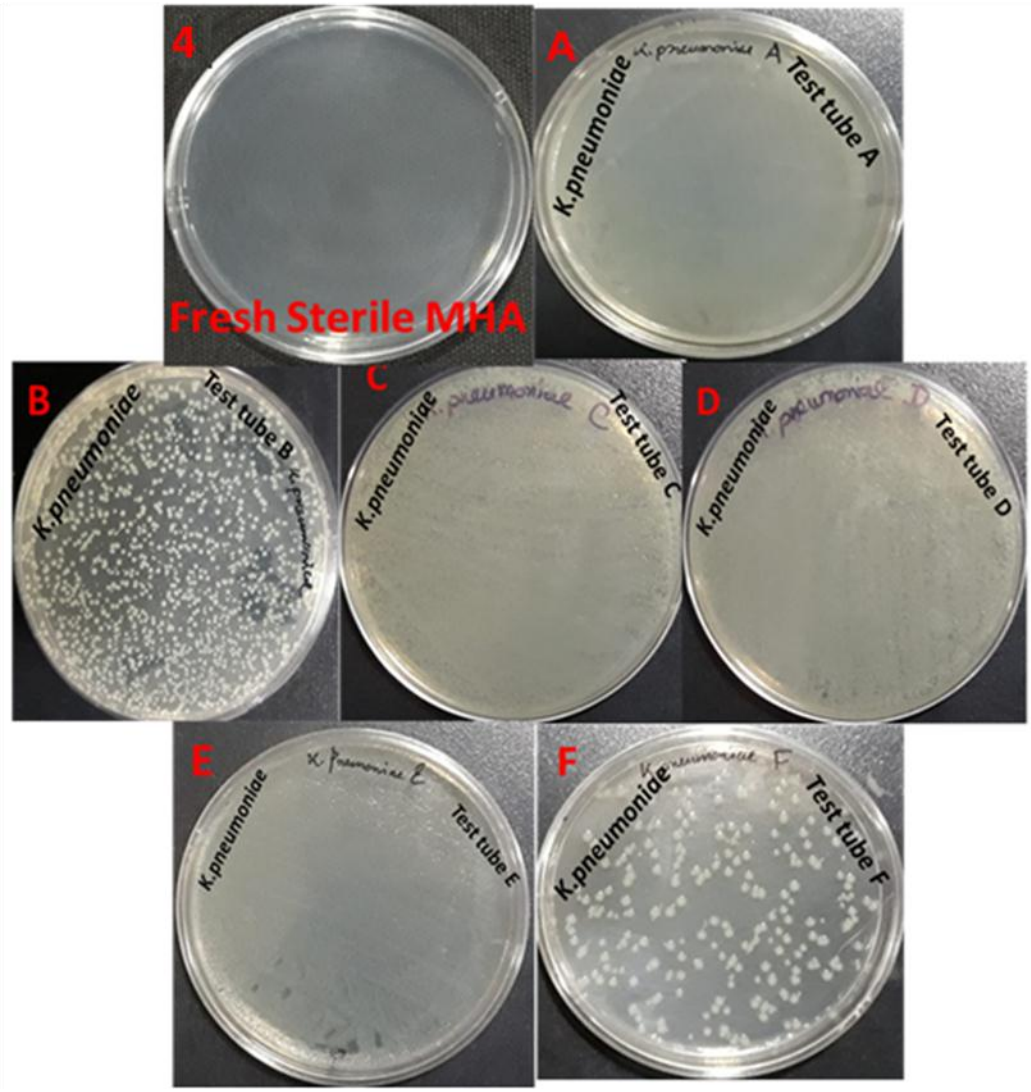

Fig 4 shows a fresh sterile Mueller Hinton Agar plate on which no colony has been grown. The translucency of this plate can be compared with the opacity of the plates with mat growth (Fig 4A, 4C, 4D and 4E).

Fig 4A shows MHA plate plated with sample from test tube A containing MHB and inoculum. This is a control set and shows profuse lawn growth of *K.pneumoniae*.

Fig 4B shows MHA plate plated with sample from test tube B containing *K.pneumoniae* with MHB and *A.alba* plant extract. This control set shows scattered growth of colonies thus indicating antibacterial efficacy of the plant extract.

Fig 4C shows MHA plate plated with sample from test tube C containing MHB, *K.pneumoniae* and ethanol (solvent used for extraction of *A.alba*) This solvent control set shows extensive mat growth of *K.pneumoniae*.

Fig 4D shows MHA plate plated with sample from test tube D containing MHB, *K.pneumoniae* and Millipore water (used for dissolving $AgNO_3$). This control set shows abundant growth of *K.pneumoniae*.

Fig 4E shows MHA plate plated with sample from test tube E containing MHB, *K.pneumoniae* and 1 mM $AgNO_3$ solution. This control set shows extensive lawn growth of *K.pneumoniae*.

Fig 4F shows MHA plate plated with sample from test tube F containing MHB, *K.pneumoniae* and *A.alba* synthesized AgNP. This test sample set shows significantly less growth of *K.pneumoniae* thus indicating high antibacterial efficacy of *A.alba* synthesized AgNP.

Image	Plate description	Volume of inoculum	No. of colonies
4	Fresh sterile MHA plate	200µl	Nil
A	Only *K.pneumoniae* inoculum	200µl	Lawn
B	**Plant extract and inoculum**	200µl	**2098±71**
C	Ethanol and inoculum	200µl	Lawn
D	Millipore water and inoculum	200µl	Lawn
E	1mM $AgNO_3$ and inoculum	200µl	Lawn
F	**AgNP and inoculum**	200µl	**98±6**

Fig. 5: UV-vis spectroscopy study of green synthesized AgNP by *A. alba*.

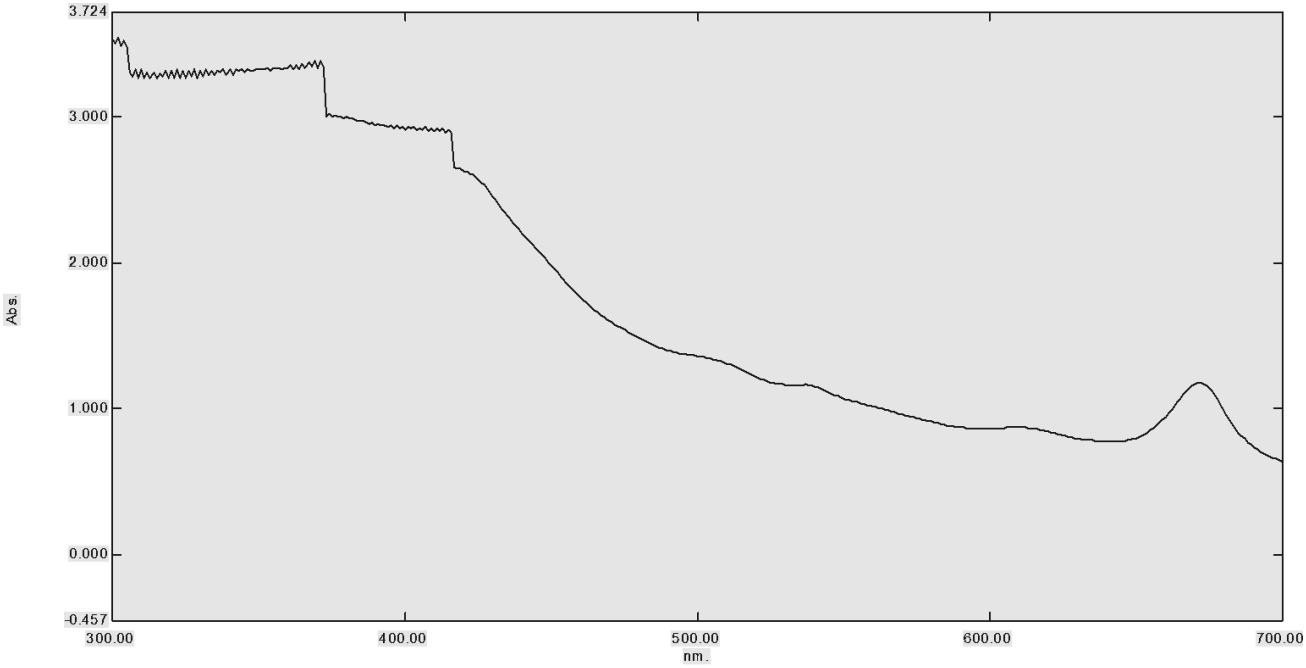

.

Peak around 420 nm (blue shift) confirms reduction of $AgNO_3$ to AgNP with particle size lesser than the reactants [47]. The ethanolic extracts of *A. alba* has reacted with 1mM $AgNO_3$ to produce silver nanoparticles. Standard used is chemically reduced 1mM $AgNO_3$ by sodium borohydride ($NaBH_4$).

Fig. 6: The FTIR of AgNP synthesized from *A. alba.* Pure plant extract of *A. alba* leaves in ethanol is used as standard.

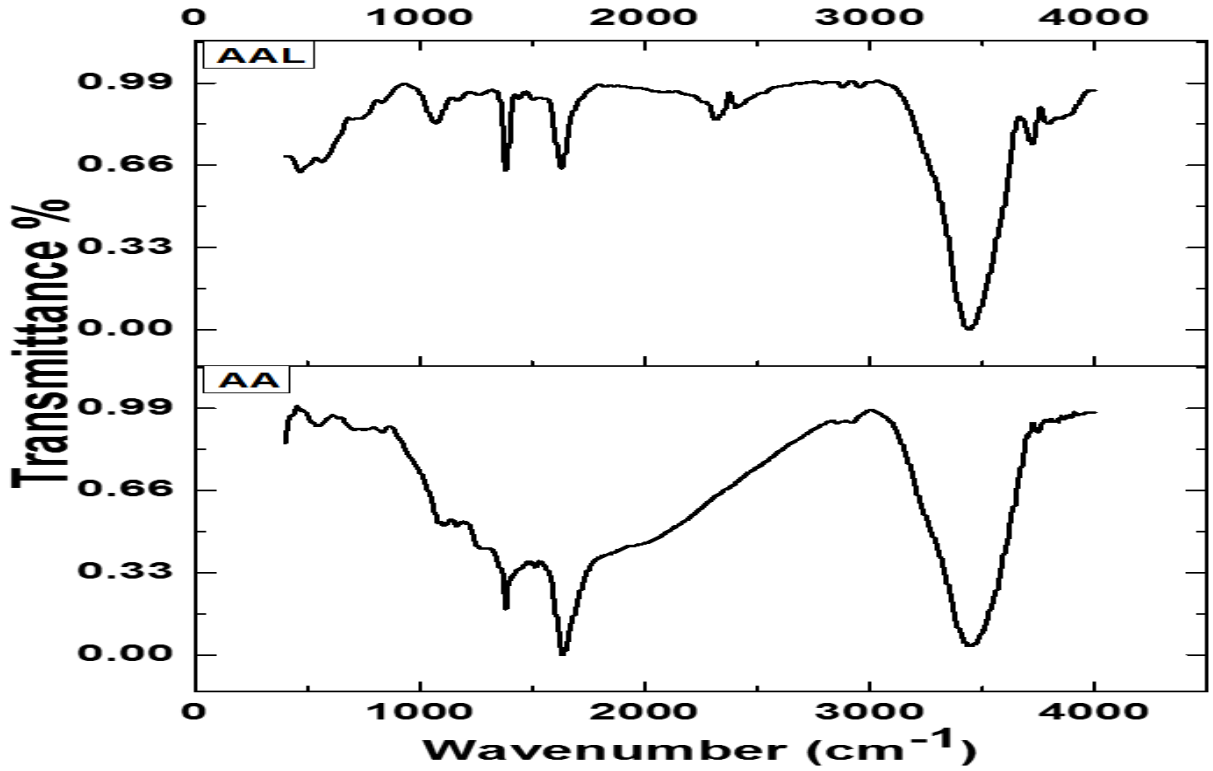

The upper graph (AAL), is the graph of *A.alba* synthesized AgNP. The graph when compared to lower graph (AA) of ethanolic extract of *A.alba* used as standard, it is seen that there is change in band size signifying involvement of secondary metabolites of *A.alba* extract in bioreduction, capping and stabilization of AgNP.

Technical support: CECRI, Tamil Nadu.

Fig 7: Comparison of the FTIR graphs of the standard (*A.alba* extract) and the green synthesized AgNP by using *A.alba* leaf extract.

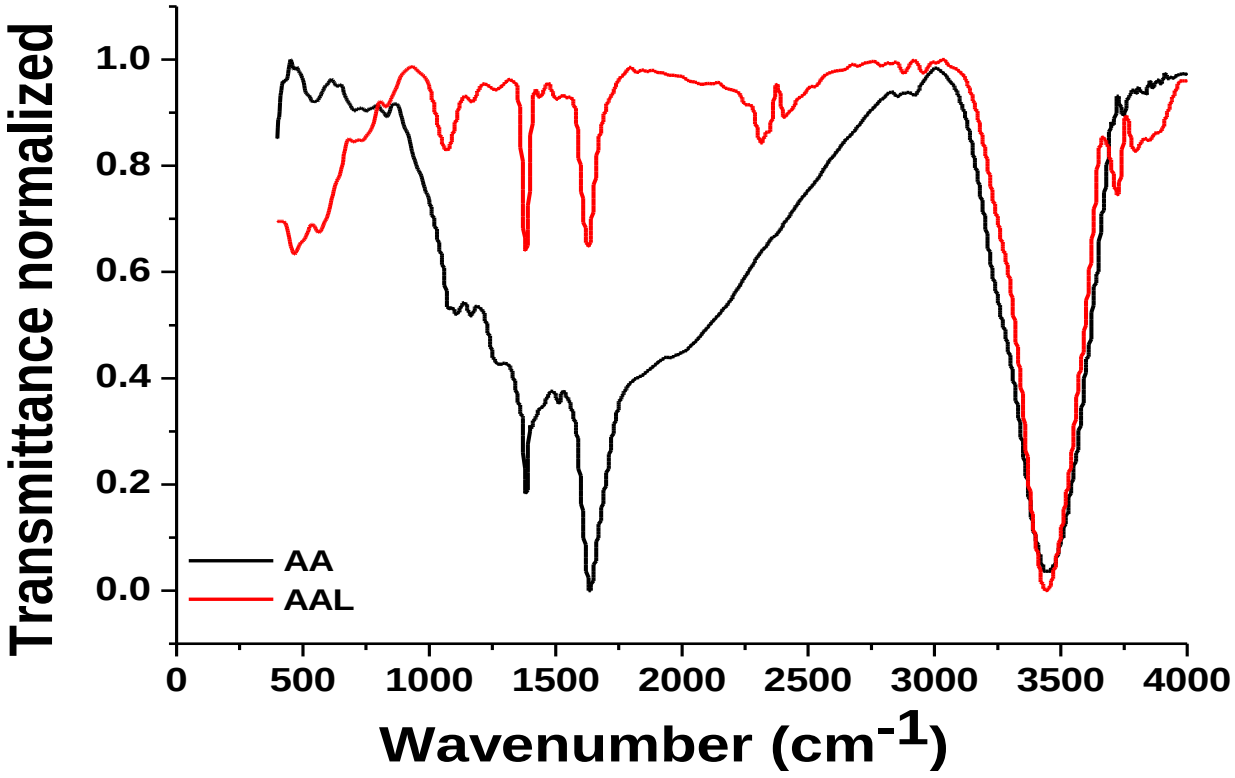

The band at 3796.24, 3723.82, 3443.41, cm^{-1} is assigned to the O–H stretching of H-bonded alcohols and phenols. The band at 2956.97, 2879.73cm^{-1} is attributed to O–H stretching of carboxylic acids. The peak value at 1629.85 cm^{-1} corresponds to N-H bonded primary amines. The peak at 2956.97, 2879.73 cm^{-1} corresponds to C-H stretch meant for carboxylic acids. The peak at 1383.07 cm^{-1} corresponds to C-N stretching of the aromatic amine group and the bands observed in 1070.55 cm^{-1} corresponds to C-O stretching of carboxylic acids, ethers, and esters. The peak at 562.71cm^{-1} corresponds to C-H stretching of the alkene group.

The signals obtained from AA (plant extract) is stronger than the signal obtained from AAL(green synthesized nanoparticles), thus confirming active participation of these molecules in bioreduction of $AgNO_3$ to AgNP.

Technical support: CECRI, Tamil Nadu.

Fig. 8: XRD- graphical representation of AgNP synthesized from *A.alba.* Standard used is 0.1mM $AgNO_3$ solution with 4 mM trisodium citrate dehydrate ($C_6H_5O_7Na_3$) as the reducing agent and 1 mM acetic acid as the capping agent.

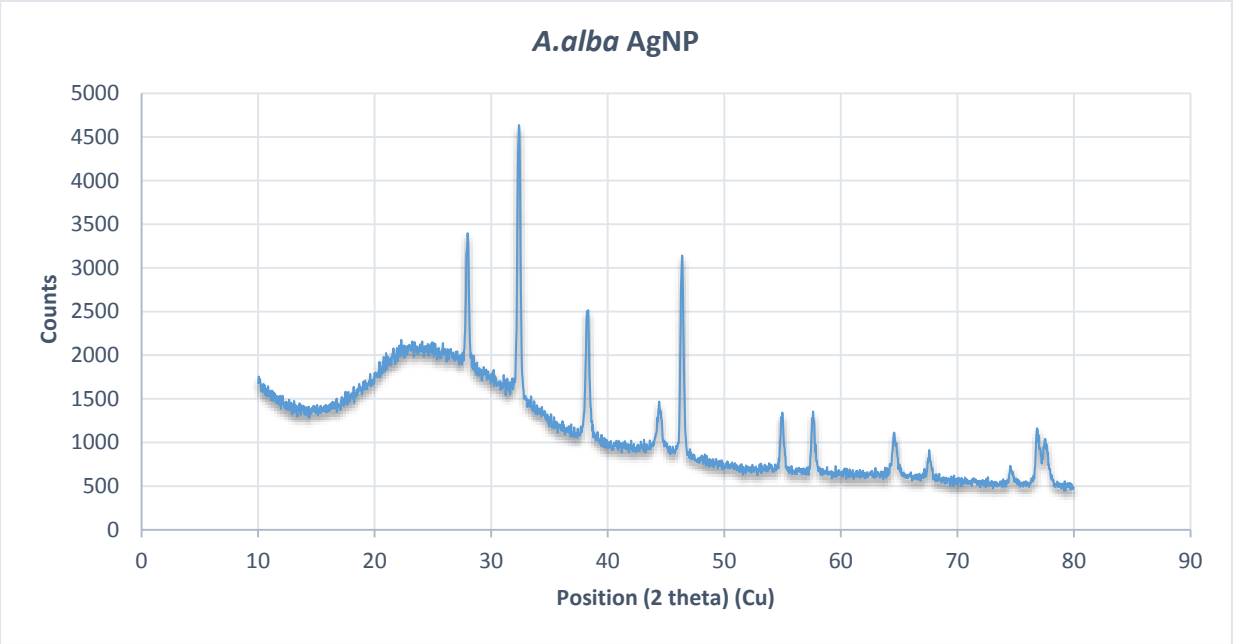

The diffraction peaksof XRD at 2θ = 32.3º, 46.3º, 64.5º and 76.8º, which can be respectively indexed to (111), (200), (220) and (311) planes of pure silver. This data associates in accordance with the powder diffraction file (PDF) no. 04-0783 pertaining to pure silver available from the Joint Committee on Powder Diffraction Standards (JCPDS) index thus representing the green synthesized AgNP have highly mono crystalline face-centred cubic (fcc) structures.

Technical Support: CLRI Tamil Nadu.

Fig. 9: TEM image of *A.alba* synthesized nanoparticles.

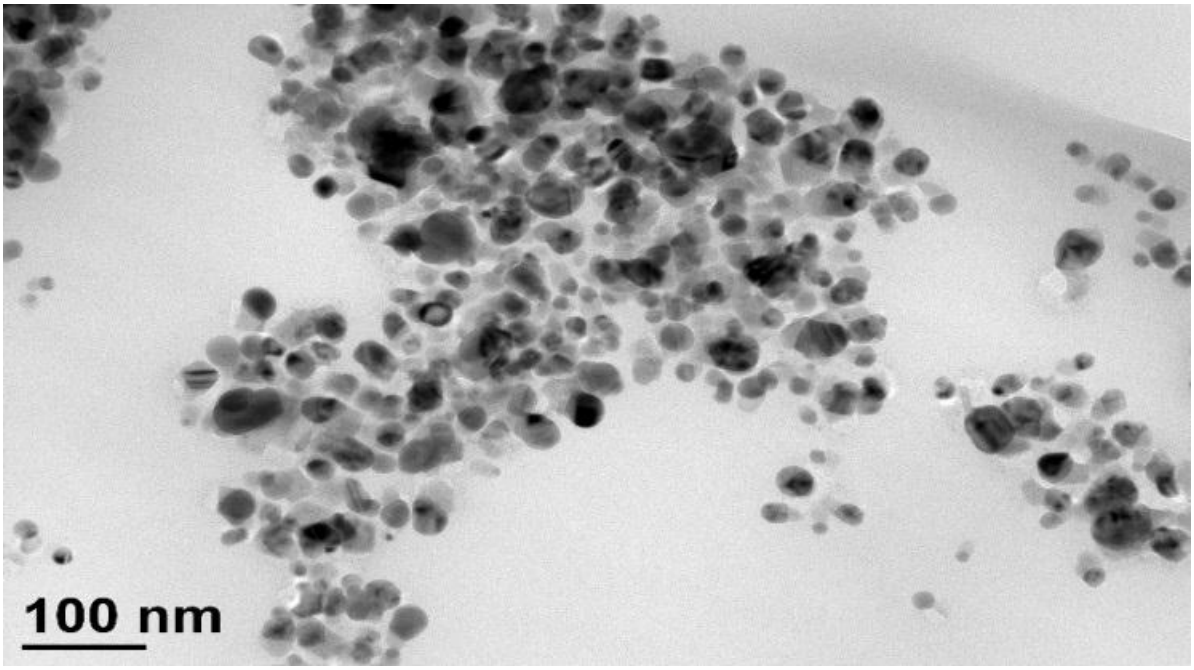

The profile, size and morphology of the synthesized silver nanoparticles were revealed by 200 keV transmission electron microscopy. The nanoparticles synthesized by *A.alba* are homogeneous and spherical which conforms to the shape of SPR band in the UV-Vis spectrum with an average diameter of 71.4 nm.

Technical support: SINP, Kolkata.

Fig. 10: SEM image of green synthesized AgNP

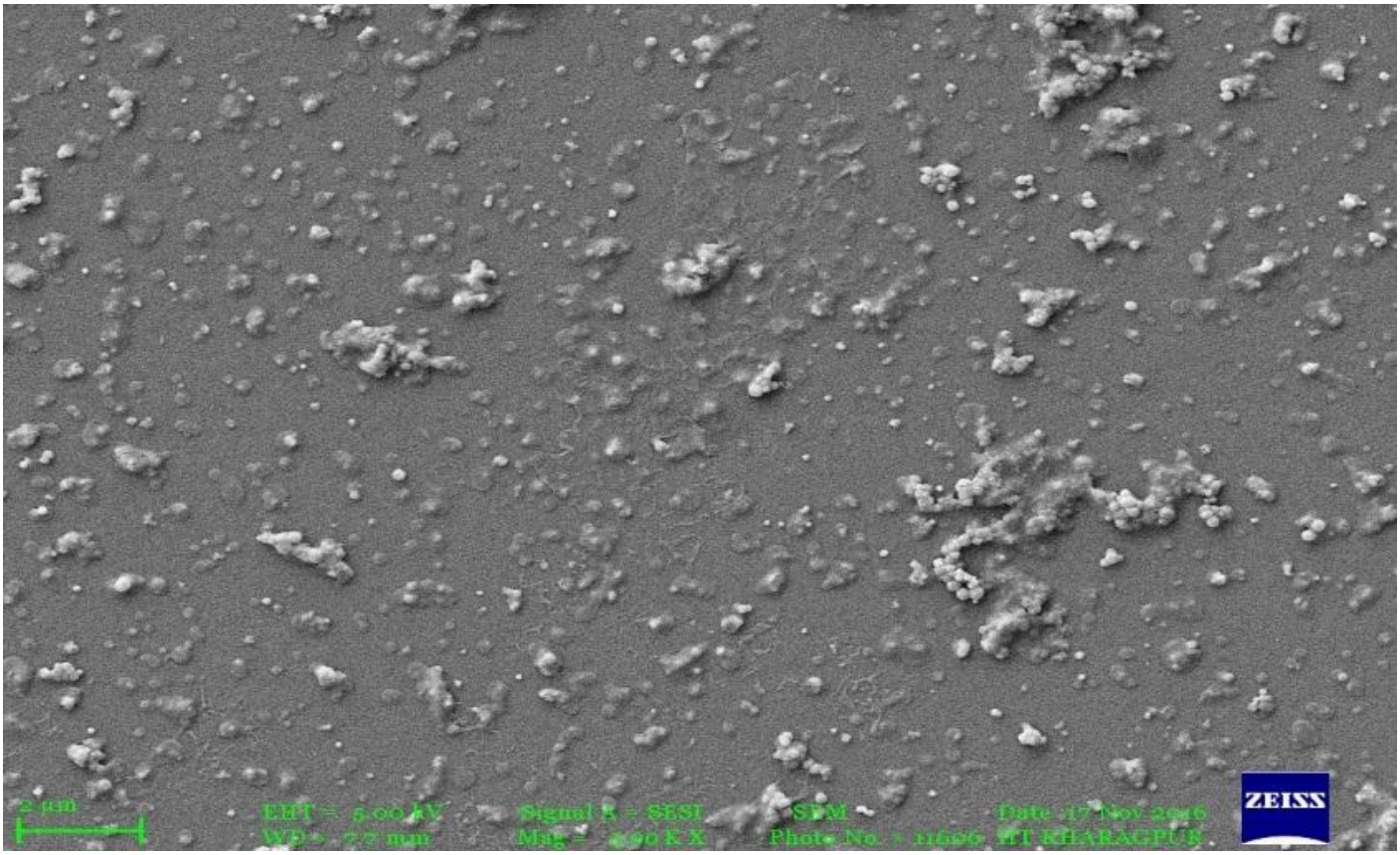

The SEM images shows fairly smooth and homogenous *A.alba* synthesized nanoparticles .

Technical Support: IIT, KGP.

Fig. 11: Cytotoxic (Hemolysis) Assay.

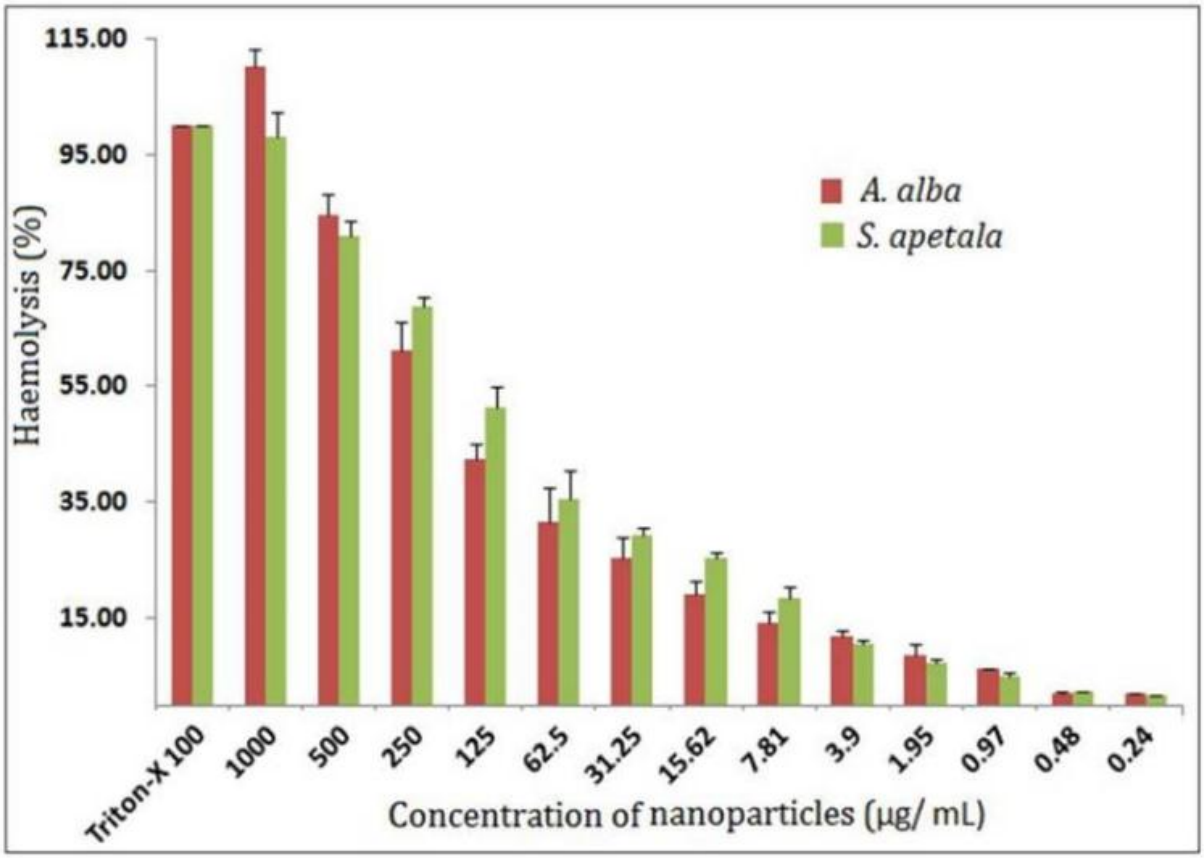

The RBCs were exposed to decreasing concentration of AgNP synthesized using *A.alba* and *S. apetala* plant extracts in a dose dependent method. Comparing with the Triton –X control (100 % lysis) it is noted that more than 15 % haemolysis could be detected in RBC treated with nanoparticle samples upto a concentration of 3.9 µg/ml. The particle synthesized from *A.alba* and *S.apetala* extracts showed no cytotoxic activity at 0.48 µg/ ml and below this concentration. So, this result indicates that nanoparticles synthesized using *A.alba* and *S.apetala* extacts are completely safe against RBCs up to a concentration of 0.48 µg/ ml. But the other nanoparticles synthesized using *C.infortunatum, A.marina* and *B. cylindrica* showed cytotoxicity beyond 0.24 µg/ml.

Technical Support: IIT, KGP.

Fig. 12: Growth curve of *E.coli* in presence of *A. alba* synthesized AgNP, ofloxacin, and their combination.

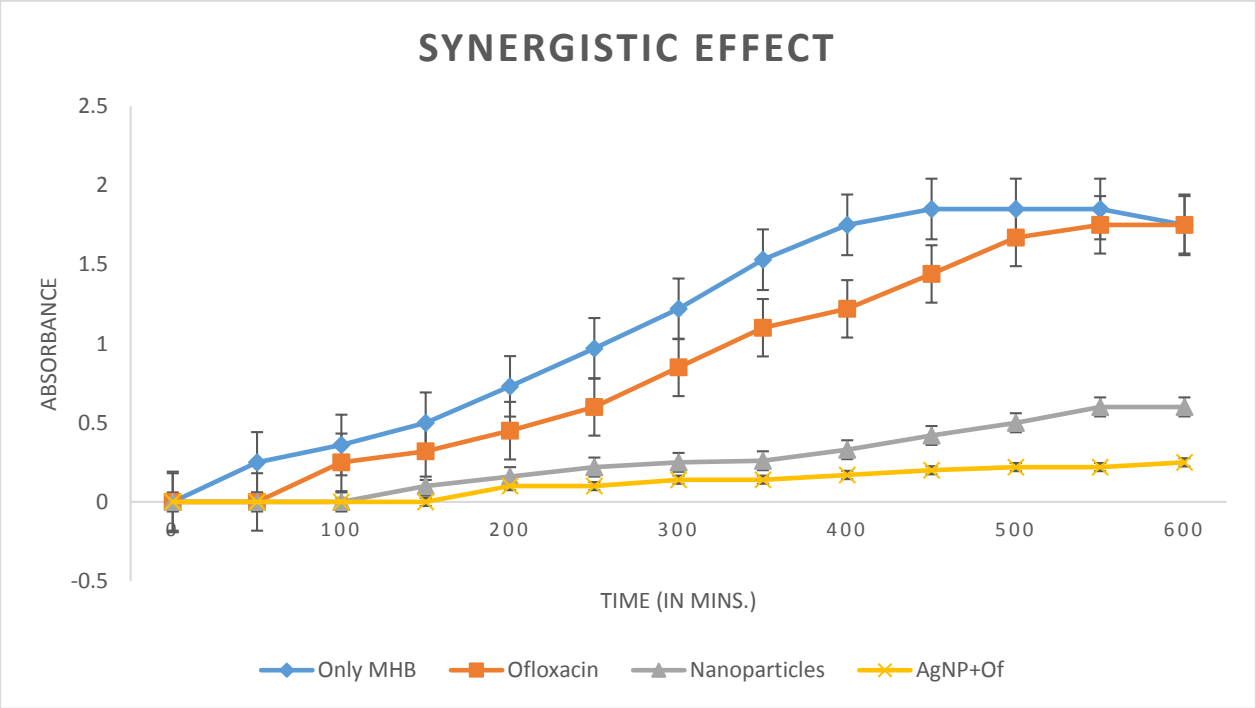

Three control setups one with only MHB and *E.coli*, second with *E.coli* in presence of Ofloxacin and third with *E.coli* in presence of nanoparticles were studied. The sample setup consisted of *E.coli* in presence of Ofloxacin (5 µg/ ml) and *A.alba* synthesized AgNP (0.48 µg/ml – the non cytotoxic dose) in synergy. The setups were incubated overnight at 37 °C and the bacterial growth curve was plotted .The absorbance was measured for 600 mins at 600nm.The experiment was repeated thrice and the results are expressed as mean of three different experiments.

Tube	Content
1	*E.coli* in only Mueller Hinton Broth
2	*E.coli* in presence of Ofloxacin
3	*E.coli* in presence of AgNP synthesized using *A.alba*
4	*E.coli* in presence of AgNP synthesized using *A.alba* and Ofloxacin

The set up with no antimicrobials and that in presence of ofloxacin (4 µg/ ml) reached log phase first, followed by the set up with nanoparticles only (at 200 mins) but no *E.coli* growth was observed in presence of conjugated nanoparticles, indicating that the conjugated nanoparticles with antibiotics in synergy can inhibit resistant pathogens in a much more effective way.

Fig. 13: Growth curve of *K.pneumoniae* in presence of *A. alba* synthesized AgNP, ofloxacin, and their combination.

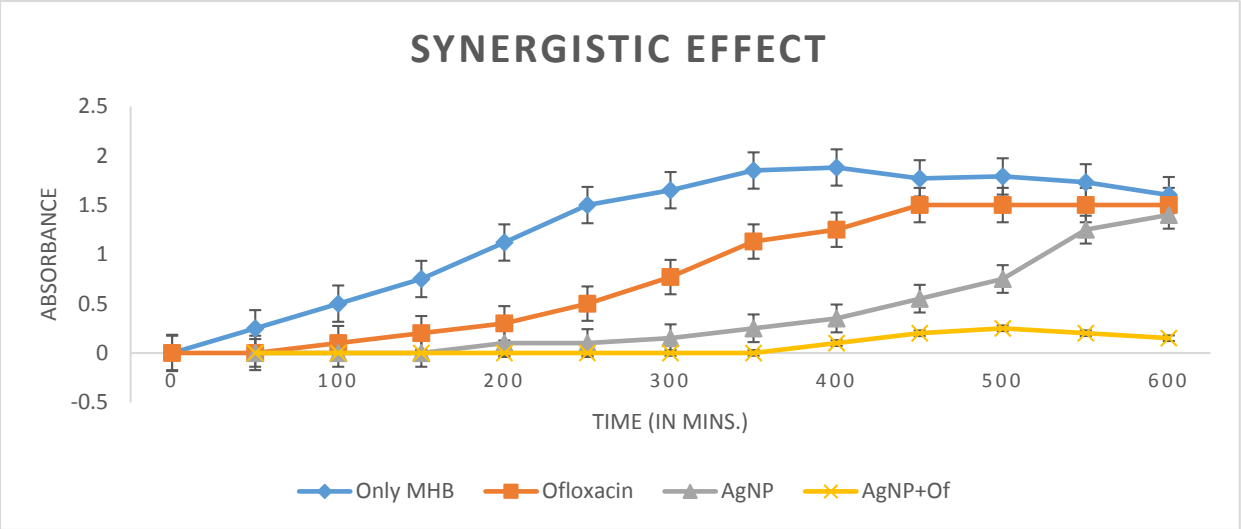

Three control setups one with only MHB and *K.pneumonoiae,* second with *K.pneumonoiae* in presence of Ofloxacin and third with *K.pneumonoiae* in presence of *A.alba* synthesized AgNP were studied. The sample setup consisted of *K.pneumonoiae* in presence of Ofloxacin (5 µg/ ml) and *A.alba* synthesized AgNP (0.48 µg/ml – the non cytotoxic dose) in synergy. The setups were incubated overnight at 37 °C and the bacterial growth curve was plotted .The absorbance was measured for 600 mins. at 600nm. The experiment was repeated thrice and the results are expressed as mean of the three different experiments.

Tube	Content
1	*K.pneumoniae* in only Mueller Hinton Broth
2	*K.pneumoniae* in presence of Ofloxacin
3	*K.pneumoniae* in presence of AgNP synthesized using *A.alba*
4	*K.pneumoniae* in presence of AgNP synthesized using *A.alba* and Ofloxacin

The set up with no antimicrobials and that in presence of ofloxacin (4 µg/ ml) reached log phase first, followed by the set up with nanoparticles only (at 200 mins) but no *K.pneumonoiae* growth was observed in presence of conjugated nanoparticles, indicating that the conjugated nanoparticles with antibiotics in synergy can inhibit resistant pathogens in a much more effective way.

Fig. 14: Growth curve of *E.coli* in presence of *S.apetala* synthesized AgNP, ofloxacin, and their combination.

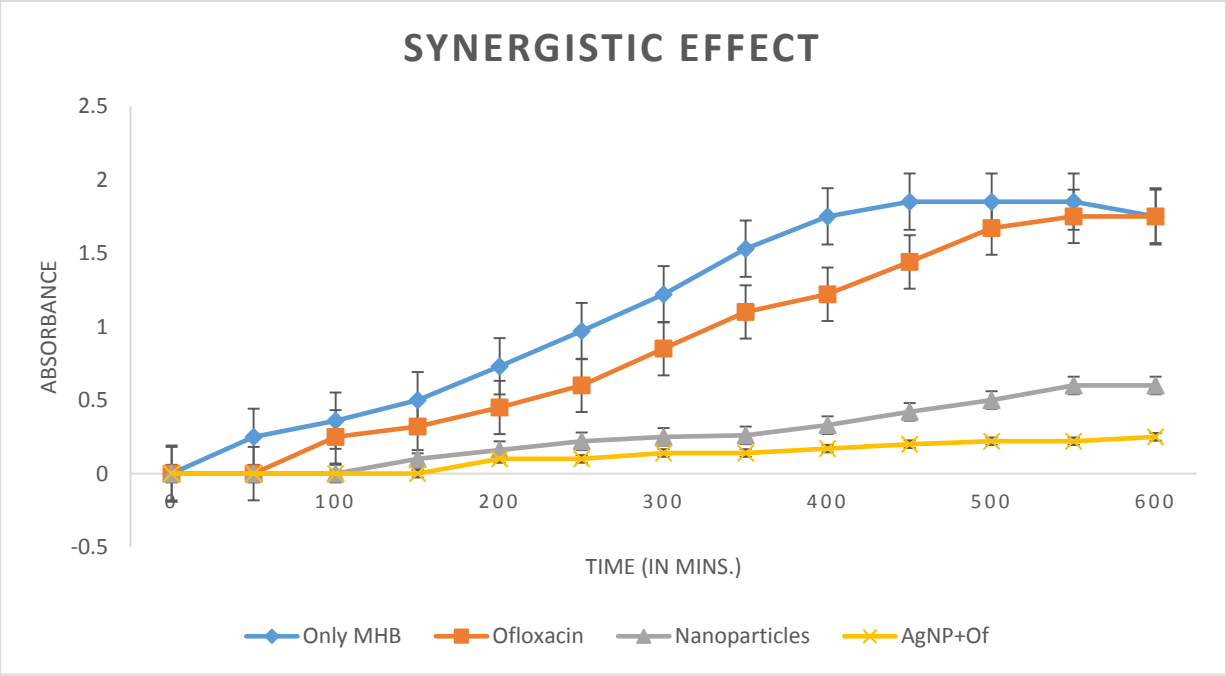

Three control setups one with only MHB and *E.coli*, second with *E.coli* in presence of Ofloxacin, third with E.coli in presence of *S. apetala* synthesized AgNP were studied. The sample setup consisted of *E.coli* in presence of Ofloxacin and *S. apetala* synthesized AgNP (0.48 µg/ml – the non cytotoxic dose) in synergy. The setups were incubated overnight at 37 °C and the bacterial growth curve was measured .The absorbance was plotted for 600 mins. at 600nm. The experiment was repeated thrice and the results are expressed as mean of the three different experiments.

Tube	Content
1	*E.coli* in only Mueller Hinton Broth
2	*E.coli* in presence of Ofloxacin
3	*E.coli* in presence of AgNP synthesized using *S.apetala*
4	*E.coli* in presence of AgNP synthesized using *S.apetala* and Ofloxacin

The set up with no antimicrobials and that in presence of ofloxacin (4 µg/ ml) reached log phase first, followed by the set up with nanoparticles only (at 200 min) but no *E.coli* growth was observed in presence of conjugated nanoparticles indicating that the conjugated nanoparticles with antibiotics in synergy can inhibit resistant pathogens in a much more effective way.

Fig. 15: Growth curve of *K.pneumoniae* in presence of *S.apetala* synthesized AgNP, ofloxacin, and their combination.

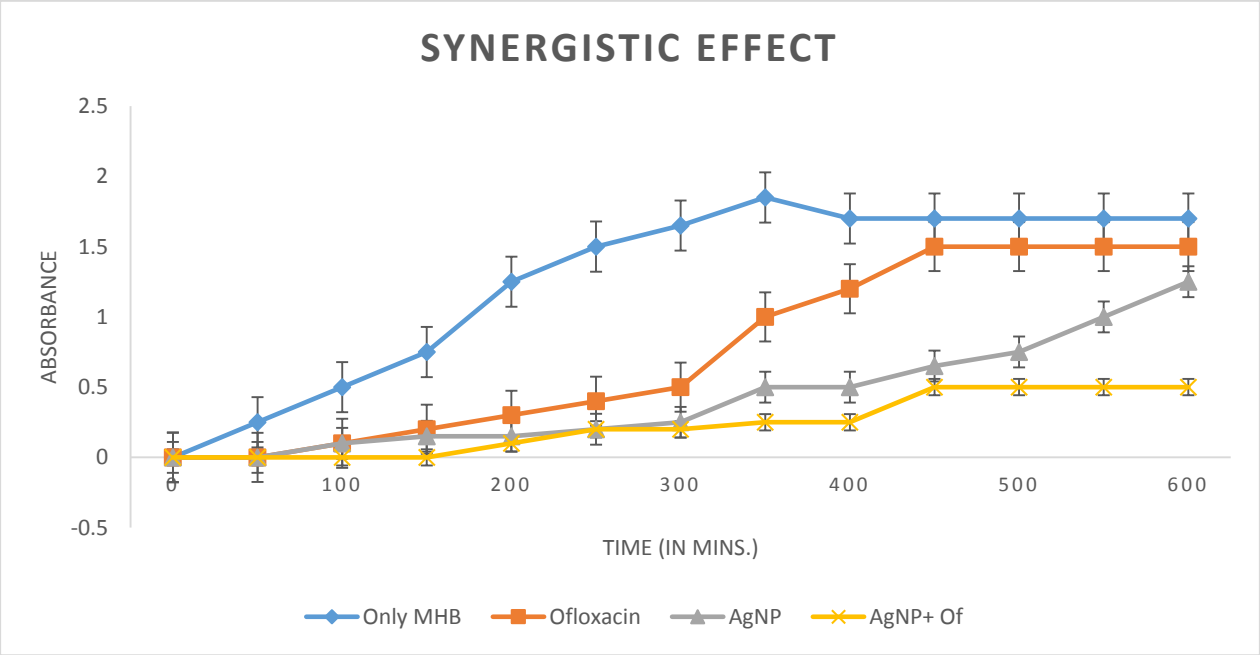

Three control setups one with only MHB and *K.pneumonoiae*, second with *K.pneumonoiae* in presence of Ofloxacin, third with *K.pneumonoiae* in presence of *S.apetala* synthesized AgNP were studied. The sample setup consisted of *K.pneumonoiae* in presence of Ofloxacin (5 µg/ ml) and *S. apetala* synthesized AgNP (0.48 µg/ml – the non cytotoxic dose) in synergy. The setups were incubated overnight at 37 °C and the bacterial growth curve was plotted .The absorbance was measured for 600 mins. at 600nm. The experiment was repeated thrice and the results are expressed as mean of the three different experiments.

Tube	Content
1	*K.pneumoniae* in only Mueller Hinton Broth
2	*K.pneumoniae* in presence of Ofloxacin
3	*K.pneumoniae* in presence of AgNP synthesized using *S.apetala*
4	*K.pneumoniae* in presence of AgNP synthesized using *S.apetala* and Ofloxacin

The set up with no antimicrobials and that in presence of ofloxacin (4 µg/ ml) reached log phase first, followed by the set up with nanoparticles only (at 200 mins.) but no *K.pneumonoiae* growth was observed in presence of conjugated nanoparticles, indicating that the conjugated nanoparticles with antibiotics in synergy can inhibit resistant pathogens in a much more effective way.

Table 1: Biochemical Assay of the selected uropathogens.

Name of Biochemical Tests	**1st uropathogen *(E.coli)***	**2nd uropathogen *(K.pneumoniae)***
Oxidase	+	-
Motility	+	-
TSI	+	+
Indole	+	-
Methyl red	+	-
Voges Proskauer	-	+
Simmmon's Citrate	-	+
Urease	-	+
Lactose fermenting	+	+
Catalase	+	+

The biochemical tests for the first uropathogen showed positive reaction for oxidase, motility, TSI, indole, methyl red, and catalase. It also fermented lactose and so, strongly indicated to be *E. coli.*

The biochemical tests for the second uropathogens showed positive reaction against TSI, Voges Proskauer, Simmon's citrate, urease and catalase. Though the second uropathogens could ferment lactose but unlike the first uropathogens they are non-motile in nature. All these tests strongly indicated the second uropathogens to be *K. pneumonia.*

Table 2: Antibiogram of the test organisms.

Strains	Diameter of inhibition zone in mm																		
	PT	Do	Ak	Cip	O	Le	Lz	Amc	Gen	Az	Ctr	Caz	To	G	Mr	Cl	Mo	Ti	C
E.coli	**15 ±1**	**20 ±0.6**	**15 ±0**	**20 ±0**	**7 ±0**	**18 ±0.6**	**6 ±0**	**8 ±0**	**15 ±0**	**19 ±0.6**	**14 ±0**	**0 ±0**	**10 ±0**	**13 ±0**	**21 ±0**	**0 ±0**	**19 ±0.6**	**0 ±0**	**25 ±0**
K.pneumoniae	**0 ±0**	**14 ±0.6**	**11 ±0.6**	**0 ±0**	**0 ±0**	**0 ±0**	**0 ±0**	**0 ±0**	**9 ±0**	**0 ±0**	**0 ±0**	**7 ±0.6**	**0 ±0**	**0 ±0**	**11 ±1**	**0 ±0**	**0 ±0**	**0 ±0**	**17 ±0.6**

PT: Pipercillin/ Tazobactum; Do: Doxycycline; Ak: Amikacin; Cip: Ciprofloxacin; O: Oxacillin; Le: Levofloxacin; Lz: Linozoid; Amc: Amoxyclav; Gen: Gentamycin; Az: Azithromycin; Ctr: Ceftriaxone; Caz: Ceftazidime ; To: Tobramycin; G: Gatifloxacin; Mr: Meropenem; Cl: Colistin; Mo: Moxycyclin; Ti: Ticarcillin; C: Chloramphenicol.

The antibiogram illustrated the sensitivity, intermediate and resistance pattern of the test organisms. *K. pneumoniae* showed complete resistance against maximum antibiotics. Only chloramphenicol and doxycycline produced clear zone and thus showing significant susceptibility. *E.coli* showed variable resistance pattern against all the antibiotics, with maximum antibiotics depicting intermediate pattern of sensitivity.

Table 3: Antimicrobial effectiveness of different ethanolic leaf extracts against *E.coli* and *K.pneummoniae* by disc diffusion method.

Name of plants	Inhibition zone (in mm) against test samples and controls			
	E.coli	*K.pneumoniae*	Ethanol (solvent control)	Streptomycin (30 µg/ml)
Euphorbia hirta	7 ±0	7 ±0	0 ±0	0 ±0
Lantana camara	9 ±0	8 ±0	0 ±0	0 ±0
Jatropha curcas	0 ±0	0 ±0	0 ±0	0 ±0
Piper betel (paan)	0 ±0	0 ±0	0 ±0	0 ±0
Justicia adhatodan (basak)	0 ±0	0 ±0	0 ±0	0 ±0
Lippia nodiflora	**12** ±0.6	**0** ±0	**0** ±0	**0** ±0
Lippia alba	**10** ±0	**0** ±0	**0** ±0	**0** ±0
Psidium guajava	7 ±0	0 ±0	0 ±0	0±0
Chlerodendrum infortunatum	**14** ±0.6	**11** ±0	**0** ±0	**0** ±0
Aegle marmalos (bael)	6 ±0	6 ±0	0 ±0	0 ±0
Cymbopogon citratus (lemon grass)	0 ±0	0 ±0	0 ±0	0 ±0
Achillea millefolium (jukti flower)	0 ±0	0 ±0	0 ±0	0 ±0
Centella asiatica (thankuni)	8 ±0	0 ±0	0 ±0	0 ±0
Andrographis paniculata (kalmegh)	9 ±1	0 ±0	0 ±0	0 ±0
Avicennia alba (lanka bain)	**16** ±0.6	**14** ±0	**0** ±0	**0** ±0
Avicennia marina (peara bain)	**15** ±0.6	**12** ±0.6	**0** ±0	**0** ±0
Brugeira cylindrical	**11** ±0.6	**6** ±0	**0** ±0	**0** ±0
Sonerratia apetala (keora)	**14** ±1	**9** ±0.6	**0** ±0	**0** ±0
Cassia fistula (bandor lathi)	8 ±0	8 ±0	0 ±0	0 ±0
Moringa oleifera (shojne)	0 ±0	0 ±0	0 ±0	0 ±0
Nyctanthes arbor-tristis (shiuli)	0 ±0	0 ±0	0 ±0	0 ±0

The plant extracts displayed bacterial inhibition patterns to varying extents depending on the susceptibility of the tested microorganisms. Out of all the leaves screened for antimicrobial efficacy all the mangrove plant extracts and two weed extracts – *C.inortunatum* and, *L.nodiflora* were most effective.

Table 4: MIC and MBC of plant extracts**.**

Name of plant Extracts	*E.coli*		*K.pneumoniae*	
	MIC (mg/ml)	MBC (mg/ml)	MIC (mg/ml)	MBC (mg/ml)
L.nodiflora	80 ±0	80 ±0	80 ±0	80 ±0
L.alba	80 ±0	80 ±0	80 ±0	80 ±0
C.infortunatum	70 ±0	70 ±0	70 ±0	80 ±0
A.alba	**60** ±0	**70** ±0	**70** ±0	**70** ±0
S.apetala	70 ±0	80 ±0	70 ±0	80 ±0
A. marina	80 ±0	80 ±0	80 ±0	80 ±0
B.cylindrica	80 ±0	80 ±0	80 ±0	80 ±0

Among all the plant extracts investigated, *A.alba* showed the least MIC value of 60mg/ml against *E.coli*, but 70mg/ml against *K. pneumonia*, followed by *S.apetala* which has a MIC value of 70 mg/ ml against both the test organisms. The MBC of *A. alba* against both the organisms were found to be 70mg/ml of the plant extracts, while most of the other extracts showed same value of MIC and MBC approving the antimicrobial effectiveness of the plant extracts.

Table 5: Total phenol and flavonoid content.

Name plant extracts	Total phenol content (mg gallic acid equivalent/ 100mg dried plant leaves)	Total flavanoid content (mg gallic acid equivalent/ 100mg dried plant leaves)
L.nodiflora	0.27 ±0.04	7.44 ±0.04
L.alba	1.0 ±0.03	10.80 ±0.10
C.infortunatum	0.8 ±0.02	16.68 ±0.08
A.alba	3.72 ±0.10	14.45 ±0.13
S.apetala	2.48 ±0.08	13.74 ±0.11
A. marina	2.17 ±0.03	13.76 ±0.07
B.cylindrica	2.36 ±0.03	13.81 ±0.08

A.alba exhibited the maximum (3.72mg gallic acid equivalent/100mg dried plant leaves) and *L. nodiflora* (0.27mg gallic acid equivalent/ 100mg dried plant leaves) showed the minimum phenolic content. *C. infortunatum* (16.68mg gallic acid equivalent/100mg dried plant leaves) showed maximum and *L. nodiflora* (7.44mg gallic acid equivalent/100mg dried plant leaves) showed the minimum flavonoid content, but all the mangrove extracts showed moderate flavonoid content. This study confirms significant antioxidant content of the plant extracts.

Table 6: DPPH Scavenging Activity

Plant Extract	DPPH Scavenging Activity (in %)
L.nodiflora	51.32 ±2.02
L.alba	69.47 ±2.92
C.infortunatum	47.71 ±1.19
A.alba	**70.02 ±1.95**
S.apetala	65.29 ±2.05
A. marina	72.86 ±2.0
B.cylindrica	63.22 ±1.97

DPPH has a maximum absorption at 517 mm. The scavenging activity of DPPH radicals by the plant extracts was examined by comparing the absorbance values of the control and the experimental tubes. The lesser the absorbance, higher is the ability of the test sample to scavenge DPPH. *A. marina* (72.84%) depicted highest scavenging activity and the lowest scavenging activity was displayed by *C. infortunatum* (47.9%).